

# The Bell System Technical Journal

Vol. XXIII

April, 1944

No. 2

---

## Indicial Response of Telephone Receivers

By E. E. MOTT

A method of analyzing telephone receiver characteristics by indicial response is discussed and illustrated by oscillograms. The indicial response of a telephone receiver is the instantaneous response of the receiver to a suddenly applied electromotive force. This type of response is of particular fundamental interest because it furnishes a key to the solution of transient problems such as are involved in the response to speech waves.

Oscillograms of indicial response, together with the more familiar steady-state frequency response characteristics, are shown for different types of receivers. The relationships existing between the two types of measurements are discussed.

From the standpoint of most faithfully reproducing transients, indicial response data indicate that a receiver having a limited range of frequency response should have a frequency response characteristic which droops gradually rather than abruptly near the upper end of the range.

### INTRODUCTION

THE use of indicial response analysis as an outgrowth of the Heaviside operational calculus<sup>1</sup> has been extended to a number of different fields. The indicial admittance as defined by J. R. Carson<sup>2</sup> in his analysis of the submarine cable and other transmission problems has been an effective tool in the study of transients. More recently, a similar type of measurement has been used as an indication of performance of amplifiers<sup>3</sup>, television equipment<sup>4</sup>, and audio frequency transformers<sup>5</sup>.

In the field of telephone receivers<sup>6</sup> an analysis by means of impressed square waves has been found useful as a measure of transient response. In the transmission of speech, so much emphasis has been placed upon steady-state frequency response as an indication of performance, that it seems in order to consider the possible advantages of a transient method of analysis, as obtained by measuring the indicial response. Only recently has the technique of such measurement been made feasible by the improvement at low frequencies of amplifiers and related apparatus.

### THE INDICIAL RESPONSE

The indicial response of a telephone receiver may be defined as the instantaneous sound pressure generated by the receiver in a closed air chamber due to a suddenly-applied unit voltage. This term differs from Carson's indicial admittance only in that sound pressure rather than current response is used. The sound pressure in an air chamber of pure stiffness is a measure

of the volume displacement, and as such it is proportional to the transfer displacement admittance of the system. When we are interested in the charge rather than in the current, the admittance takes the form of a displacement admittance, related to the ordinary admittance by a factor of the frequency  $\omega$ . That Carson's original equations apply to such a system with little if any change may be easily demonstrated. The term  $A(t)$  may be used to denote any of these forms of indicial admittance or indicial response.

The form of the applied voltage assumed is shown by Fig. 1. This form, defined by Heaviside as the *unit function*, is a function of time equal to zero before, and unity after the time  $t = 0$ . More properly, however, it may be regarded as an increment in voltage closely analogous to Isaac Newton's concept of infinitesimal elements of rectangular area, the summation of which forms the basis of the integral calculus. The successive application of small increments of voltage likewise forms the basis of the operational calculus, or more particularly, the basis of the Carson extension theorem.

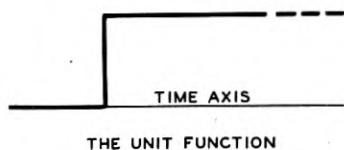


Fig. 1

#### THE CARSON EXTENSION THEOREM

\* Having obtained the indicial response, either experimentally or theoretically, we have the key to the more general problem where the applied voltage  $e(t)$  may be of any form, such as that of speech waves. Let  $e(t)$ , Fig. 2, be any arbitrary voltage wave corresponding to speech<sup>7</sup>. Let a series of consecutive increments of voltage, differing in time by  $\Delta\tau$  be applied, of such magnitude as to build up the form of the curve  $e(t)$ . By analyzing each of these components in terms of the indicial admittance  $A(t)$ , and synthesizing them again, the instantaneous sound pressure may be related to the voltage producing it and the indicial admittance  $A(\tau)$  by the Carson extension equation<sup>2</sup>:

$$p(t) = \frac{d}{dt} \int_0^t A(\tau)e(t - \tau) d\tau$$

When the above integration is carried out, the term  $\tau$  disappears and is replaced by  $t$ . The above sound pressure  $p(t)$  represents the sound pressure generated by the receiver in a closed coupler due to an applied voltage  $e(t)$ .

$$p(t) = \int_0^{\infty} A(\tau) e(t-\tau) d\tau$$

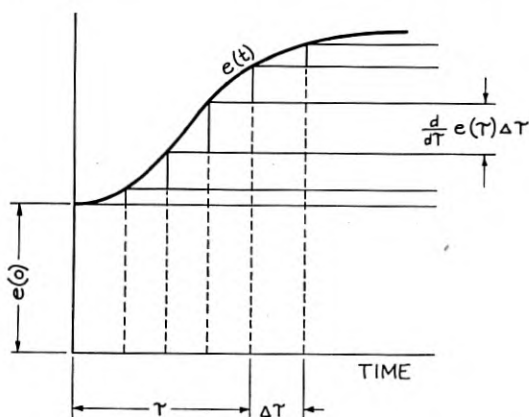


Fig. 2—Method of derivation of Carson's extension formula.

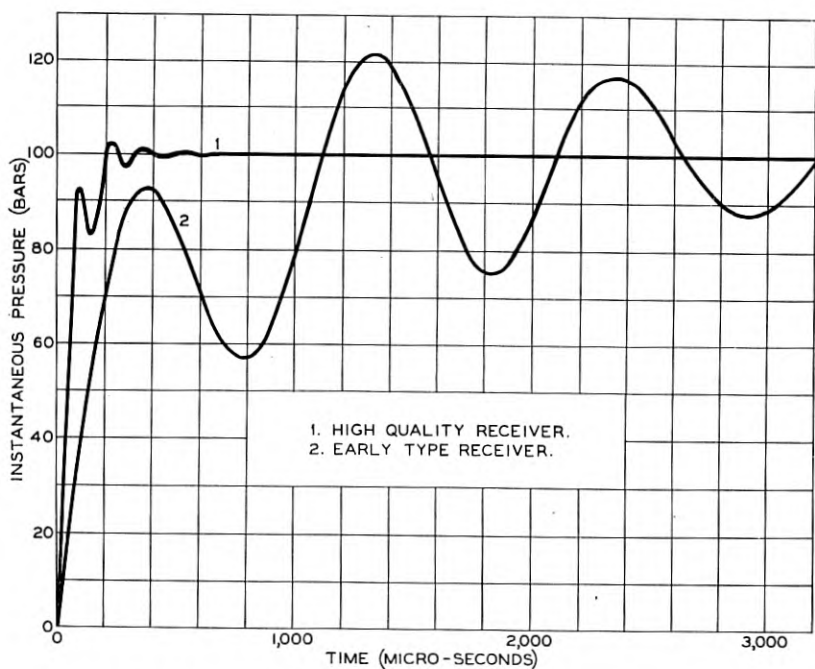


Fig. 3—Indicial admittance of two types of telephone receivers.

From the above, it is evident that the ideal form of receiver response to a suddenly-impressed voltage would be a copy of the unit function shown in Fig. 1, and that any deviation from this form will cause distortion. If the building blocks of the curve  $e(t)$  are undistorted, the curve itself will likewise be reproduced free from distortion of wave form. Thus, the more closely the indicial response can be made to approach the form of the unit function, the more closely the receiver sound pressure  $p(t)$  will be a copy of any arbitrary speech wave  $e(t)$ . Curve 1, Fig. 3, shows the indicial response of a receiver having a frequency range of 8000 cps, which comes rather close to this ideal. On the other hand, the further the indicial response departs from this ideal form, the more it will deviate from any impressed transient, such as speech waves. Thus curve 2, Fig. 3, corresponds to a receiver of narrow range, which contains resonant oscillations, and rises much later in time than the other receiver.

#### CONVERSION FORMULAE

The indicial response is as fundamental in character as frequency response, and may be converted into frequency and phase response if the proper integrations are carried out for any particular system, as follows:

$$\text{Indicial Response } A(t) \Leftrightarrow \left[ \begin{array}{l} \text{Frequency Response} \\ + \text{Phase Response} \end{array} \right] A(\omega) = P(\omega) + jQ(\omega)$$

where  $A(\omega)$  is the transfer admittance of the system. In order to carry out these conversions, certain integrations must be performed, either mechanically or theoretically. The following are conversions<sup>7</sup> which may be used to carry out this process:

$$A(t) = \frac{2}{\pi} \int_0^{\infty} \frac{P(\omega)}{\omega} \sin \omega t d\omega$$

$$A(t) = P(0) + \frac{2}{\pi} \int_0^{\infty} \frac{Q(\omega)}{\omega} \cos \omega t d\omega$$

$$\frac{P(\omega)}{\omega} = \int_0^{\infty} A(t) \sin \omega t dt$$

$$\frac{Q(\omega)}{\omega} = \int_0^{\infty} [A(t) - A(0)] \cos \omega t dt$$

Where  $P(\omega)$  and  $Q(\omega)$  are the real and imaginary parts of the frequency response,  $A(\omega)$  is expressed in terms of pressure response<sup>8</sup>, while the indicial response  $A(t)$  is expressed as an instantaneous sound pressure. The integrations are difficult to carry out, but serve to show how the two systems of

measurement are related, and how they may theoretically be converted one into the other, provided in the case of frequency response the magnitude and phase are both known.

### GENERAL APPLICATIONS

The use of indicial response as a tool in telephone receiver studies is particularly adapted to the study of transients. Since all voice and sound transmission, particularly that of orchestral music, may be regarded as essentially a transient problem, it is appropriate that we visualize the effects on the complex wave forms of any distortions which may be present in the transmission apparatus. The indicial response will, in general, depart from the ideal square form, and the amount of this departure may be regarded as indicative of the relative faithfulness of wave form reproduction by apparatus having different frequency characteristics. An examination of these departures should therefore be helpful as a supplementary method of appraising the relative merits of different frequency response characteristics. The effect, for example, of small resonance peaks or dips upon transients is very forcefully shown in the form of the indicial admittance. The departure from squareness of a particular system may often be improved by use of the proper shape of frequency characteristic.

The use of a closed coupler when measuring telephone receivers is particularly adapted for such studies, because the disturbing effects of deficiencies at the low frequencies due to leakage may thus be eliminated. Interpretation by inspection then becomes a matter of observation of the various types of departures at the higher frequencies from the ideal form.

Since listening tests do not always agree with interpretations of physical measurements of steady-state frequency response, it often becomes a matter of interest to obtain different criteria of judgment in which the weight given to the various frequencies may be judged by the relative effects of irregularities in various parts of the frequency spectrum upon the indicial response.

### APPARATUS AND METHOD OF TESTING

Various forms of apparatus may be used for receiver testing with square waves. Square-wave generator circuits have been published both for audio<sup>5</sup> and video<sup>3</sup> frequency use, involving vacuum tube circuits which overload at low voltages. For low speeds using low-frequency waves of the order 60 cps, a simple mercury switch operated by an oscillator gives very satisfactory results.

The square-wave voltage is introduced across a small part of the resistance termination as shown in Fig. 4, the whole resistance termination being matched to the magnitude of the receiver impedance at 800 cps. The re-

ceiver is then operating from an idealized resistance source having an impedance which matches that of the receiver approximately, over the range of interest.

The receiver is coupled acoustically to a small-diameter condenser microphone by means of a closed coupler<sup>8</sup>. The condenser microphone has a substantially uniform characteristic up to a frequency of 10 kc. The

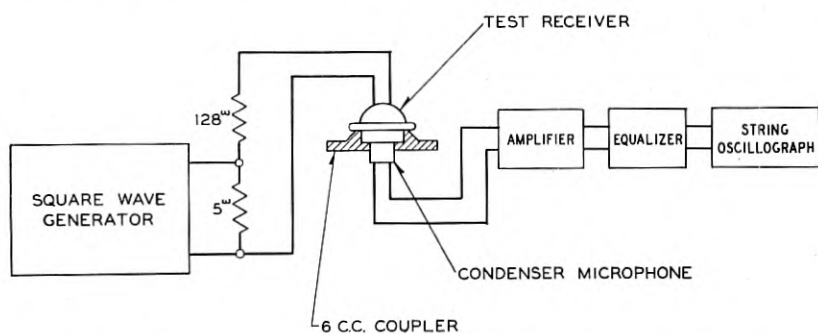
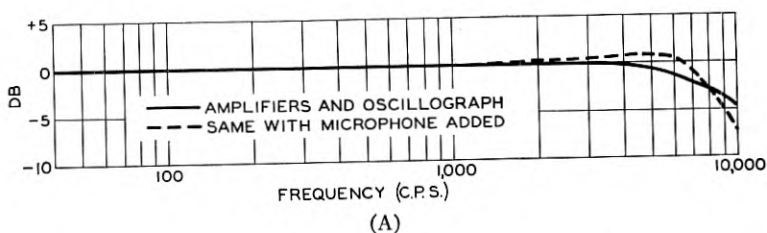


Fig. 4—Circuit diagram of apparatus for indicial response measurements.



(B)

Fig. 5—Frequency response (A) and indicial response (B) of measuring apparatus.

microphone voltage is then amplified to the point where it can be measured by an oscillograph.

Either the cathode-ray oscilloscope or a rapid-recording string oscillograph<sup>9</sup> may be used, but in the latter case it is necessary to equalize the string oscillograph to a frequency of about 10 kc in order to cover the audio frequency range. The choice of these instruments depends somewhat upon whether a permanent record is desired or whether a visual indication is sufficient.

The amplifier must be compensated at low frequencies in order to maintain a strictly square-wave output. The entire system characteristic is shown in Fig. 5 and covers a range of 1 to 10,000 cps with a substantially uniform frequency response. The indicial response of the system is also shown to be reasonably free from irregularities. Such irregularities as do exist are due largely to the sharp cut-off of the system at 10 kc which was necessitated by the limitations of the string oscillograph.

#### INDICIAL VS. FREQUENCY RESPONSE

The calculated pairs of curves for telephone receivers in Fig. 6 show the relations between the frequency response and the indicial response. Since the characteristics of receivers measured on a closed coupler of known volume are readily amenable to calculation if the constants of the receiver are known, such a procedure is often useful in predetermining the design of a receiver.

The upper three curves, Fig. 6, are the characteristics of a moving coil receiver calculated for three different frequency ranges, being otherwise similar in shape, the curve being shifted in frequency by an arbitrary factor  $K$ . The effect on the indicial admittance is to shift it in time by the same factor without change of shape, if the plot is logarithmic as shown. In general, if the cut-off frequency is divided by the factor  $K$ , the corresponding time delay will be increased by the factor  $K$ . This is an application of a theorem by Carson<sup>2</sup> that:

$$\frac{1}{pZ(kp)} = \int_0^{\infty} A(t/k)\epsilon^{-pt} dt$$

where  $p = j\omega$  is proportional to frequency, and  $t$  is the time,  $\frac{1}{Z(kp)}$  is the frequency response, and  $A(t/k)$  is the indicial response. In other words, the curve may be shifted in frequency by a simple transformation and the effect on the indicial admittance curve is very similar except that the shift is in a direction opposite to the change in frequency, and is inversely proportional to the change in frequency scale.

The second group of curves, Fig. 6, relates to the effect of damping on an early magnetic type of receiver, showing the freely resonant condition, a moderately damped, and a highly damped receiver. The curves of indicial response show the effects of free resonance to be very detrimental, and the ringing of the diaphragm is sustained over such a long period that any speech waves would have superposed on them a continual train of sine waves. If the rate of decay of these waves is increased, as shown by the damped curves, a noticeable improvement results. By using critical damping as in the highly damped curve, all oscillations can be eliminated, but the time of pickup is degraded and the departure from a square wave is somewhat greater than for the moderately damped condition.



The indicial response shows more emphatically than frequency response, the importance of damping and the oscillations which are to be avoided, or reduced to a minimum. It also shows that the effect of delay is closely related to attenuation of the higher frequencies, and that frequency of cut-off is inversely proportional to the time delay, for a given type of receiver circuit.

There is a noticeable similarity between the appearance of the frequency response and the indicial response curves, and in many cases one curve is approximately the image of the other. As an example of this, the three pairs of linear curves show the similarity of indicial and frequency response for constant velocity, constant acceleration, and constant amplitude devices, as depicted by the three curves denoted by 1, 2, and 3 in which the three moving-coil instruments are assumed to be controlled by (1) a predominance of acoustic resistance behind the diaphragm, (2) a mass controlled system, and (3) a stiffness controlled system. In either case, the fundamental shape of the curves is such that the indicial response is the image of the frequency response in its general character.

The two lower curves, Fig. 6, indicate the effect of a sharp cut-off versus a gradual one. In terms of indicial response, the gradual cut-off appears to be the better of the two, a principle which is widely accepted in television and telegraph transmission.

#### EXPERIMENTAL MEASUREMENTS

The oscillographic measurements of indicial response, together with corresponding frequency response measurements of telephone receivers, are shown in Figs. 7, 8, and 9. The oscillograms on the left, Fig. 7, show the type of data which constitute indicial response as compared with the more familiar frequency response on the right.

Curve 1, Fig. 7, represents a moving-coil receiver similar to that calculated in Fig. 3, and constitutes the standard of performance which can be obtained by this particular system of measurement. Each division of the oscillogram represents .001 second, a somewhat faster film speed than is usual for the string oscillograph.

Curve 2 shows the characteristics of a magnetic bipolar type of receiver having a frequency range of 3000 cps with a fairly sharp cut-off at this frequency. The acoustic circuits of this receiver serve to damp the resonance of the diaphragm and extend the range from 1600 up to 3000 cps. The oscillogram shows a partially damped but still somewhat oscillatory condition which is due to the receiver.

With all damping circuits removed, we obtain the characteristic of curve 3, a simple diaphragm resonance, which is similar to the earlier type of receivers of the magnetic type. Curve 2 represents a real improvement over

curve 3, both as regards introduction of damping and extending the frequency range.

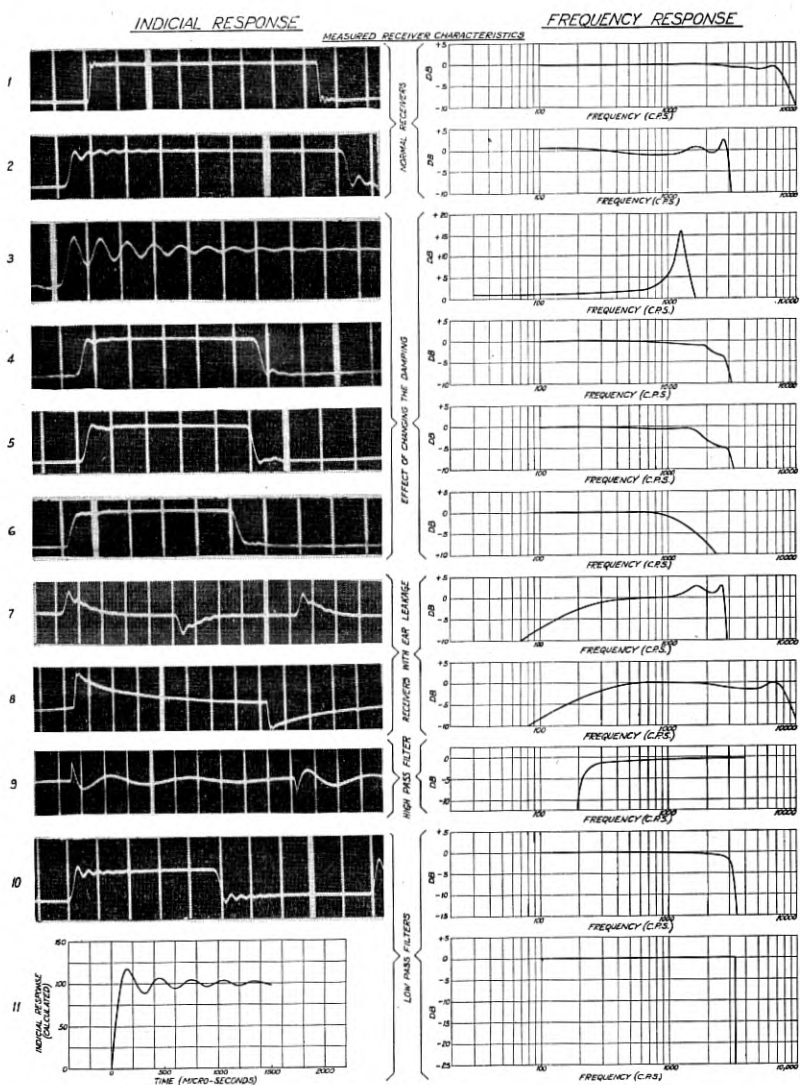


Fig. 7—Measured indicial response versus measured frequency response of various types of telephone receivers and electrical filters.

The effects of further increases in damping are shown by curves 4, 5, and 6. Such changes in the shape of the curve are brought about by relatively simple

changes of the constants of the acoustic circuits. The oscillograms indicate a marked improvement as regards oscillations, which is to be expected with increased damping. The time delay is eventually degraded with further increases of damping, however, and the optimum damping is a matter of compromise.

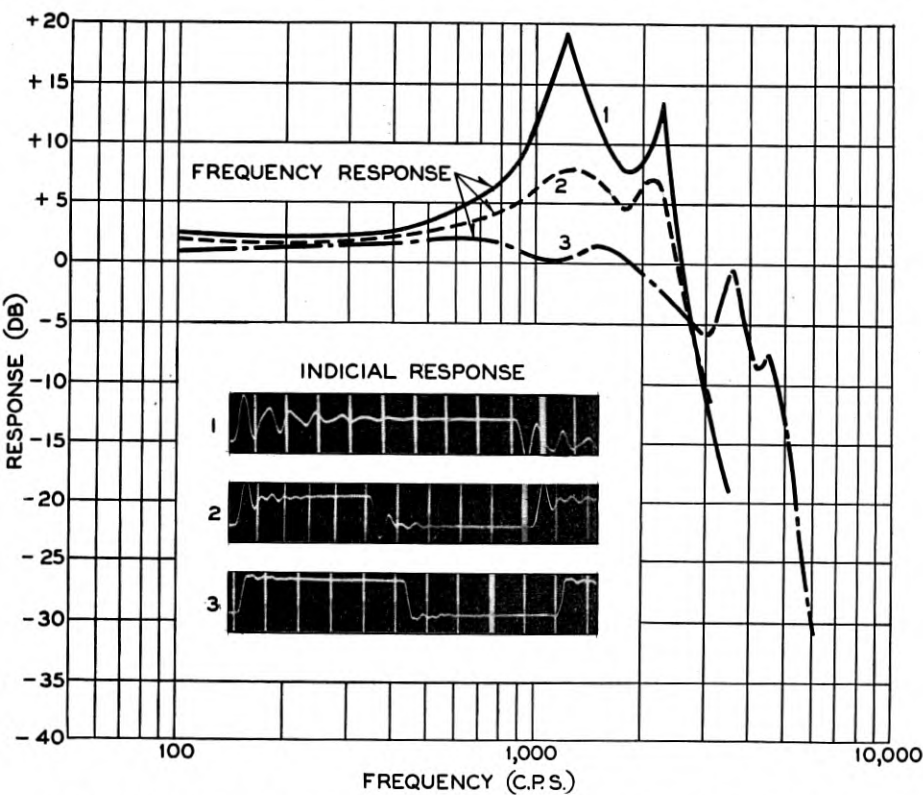


Fig. 8—Three types of hearing aid receivers—frequency response and indicial response.

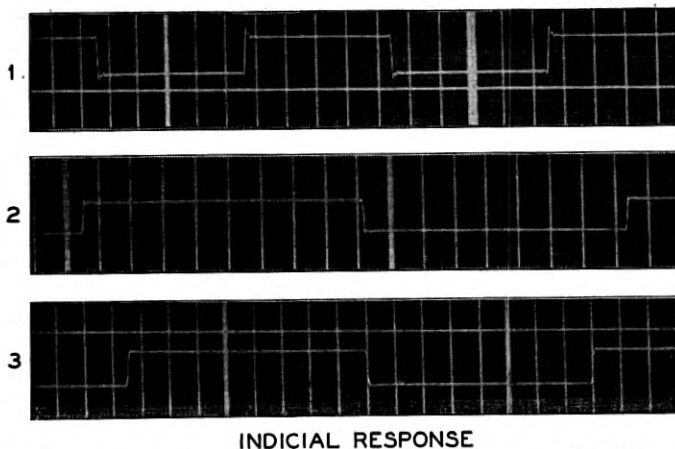
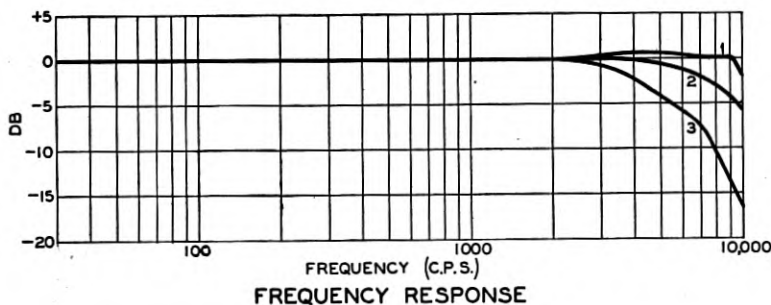
The effects of a low-frequency cut-off characteristic are shown by curves 7, 8, and 9, Fig. 7. The absence of a *d-c* component makes these curves very difficult of interpretation.

Curve 7, taken with the same receiver as curve 2, except with coupler leakage, shows a loss at low frequencies which is typical of cases where the receiver cap does not make a perfect seal with the ear. The effect on the indicial response is that of a large pulse followed by a few oscillations at the frequency of the leak circuit.

Curve 8 is a similar condition except taken on a high-quality receiver

circuit. This also shows a similar effect. The initial pulse contains most of the receiver characteristic, while the curve which follows is mainly dependent on the leakage constants.

Curve 9 is taken on a high-pass filter of the characteristic shown. It may be proved that this curve is the inverted image of the corresponding low-pass filter characteristic, of which a similar curve is shown as curve 10.



#### INDICIAL RESPONSE

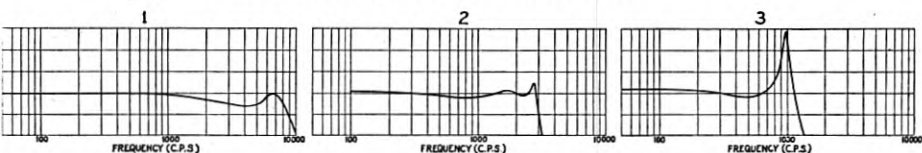
Fig. 9—String oscillograph characteristics—frequency response and indicial response with different amounts of damping.

The curves 7, 8, and 9 show that when the low frequencies are absent, the indicial response becomes too difficult to interpret. We must restrict our measurements to systems which are ideal at the low frequencies in order to interpret the indicial admittance by inspection.

Curves 10 and 11, Fig. 7, are low-pass filter characteristics, the former being a measured curve of a typical filter, while the latter is a calculated curve for an ideal filter. The two curves check reasonably well and indicate the effect of a very sharp cutoff as compared to those of the receivers shown

above. This indicates the oscillatory nature of any system having a sharp cutoff at the upper frequencies.

## FREQUENCY RESPONSE OF TELEPHONE RECEIVERS



## SQUARE WAVE RESPONSE

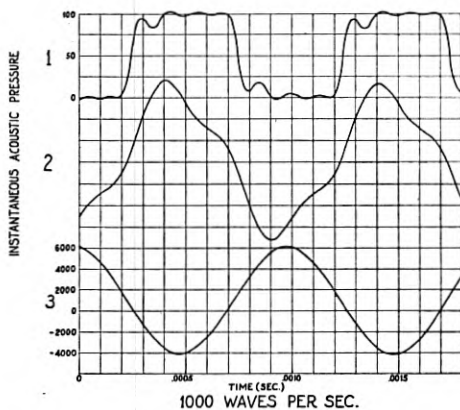
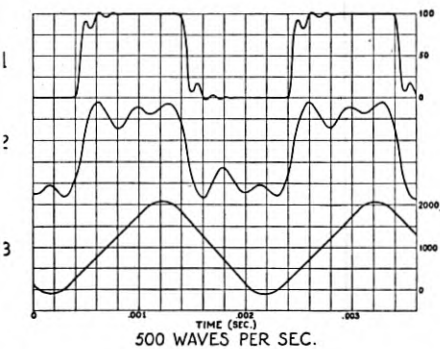
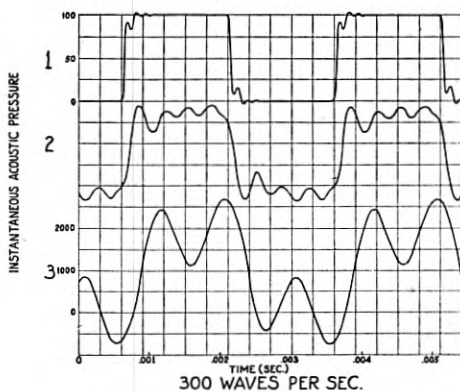
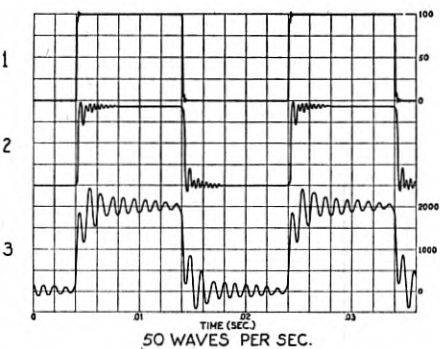


Fig. 10—Transient response to square waves of three different types of telephone receivers denoted by Nos. 1, 2 and 3, whose frequency response characteristics are shown above. Note the change in each type of pattern as the frequency of the square waves is increased.

Figure 8 shows a group of curves of the frequency response and indicial response of a group of receivers used as hearing aids. Curve 1 shows a very efficient but resonant receiver. Curve 2 is somewhat damped but still contains oscillations. Curve 3 is comparatively much better than either of the others from an indicial response viewpoint, and has a drooping frequency response characteristic, and demonstrates the advantages of this form of curve.

Figure 9 shows the effect of adding damping to the system of the string oscillograph when subjected to an ideal square wave. Curve 1, which has a virtually flat characteristic from 1 to 10,000 cps, is characterized by a sharp oscillatory peak in the indicial response. Curve 2 contains some oscillations, while curve 3 is substantially free from oscillations. The trend of these curves also shows the more faithful reproduction of transients obtained with a drooping frequency response.

Figure 10 shows the response to square waves of three receivers having different frequency response characteristics. The low-frequency waves of 50 cps are similar to the indicial response of the three receivers whose frequency characteristics are shown at the top, Fig. 10. As the frequency of these waves is increased to 300 cps, a noticeable departure from the square form is apparent in receiver No. 3. Receiver No. 2 shows a slight departure, while No. 1 is virtually a perfect reproduction.

As the frequency of the square waves is increased to 500 cps, the receiver No. 1 still shows very little departure from the original form. Receiver No. 2 maintains a fair approximation, while receiver No. 3 has lost all resemblance to the square form.

At a frequency of 1000 cps, only the first receiver maintains an approximately square form. Receivers Nos. 2 and 3 have both lost their identity and have become practically pure sinusoids. For all higher frequencies of the square waves, these two receivers will exhibit practically pure sinusoidal forms, due to the relatively sloping character of the frequency response at these frequencies, and the absence of harmonics. The same will be true of receiver No. 1 beyond a frequency of 3000 cps.

It will be realized, of course, that the patterns were obtained with square waves repeated at frequencies of 50, 300, 500 and 1000 cycles per second. While some speech waves approximate square waves in character such waves, when they occur, are repetitive only at the lower range of these frequencies. The above patterns were therefore obtained under conditions much more severe than are involved in the reproduction of speech waves and are included primarily for the purpose of illustrating the sensitivity of this form of analysis when applied to repeated square waves.

## CONCLUSIONS

To summarize these data, it seems evident that square wave analysis may be applied in some fields of acoustics for both theoretical and practical applications.

In theory, the indicial response forms a somewhat different approach to the problem of obtaining the optimum characteristics of telephone receivers at the upper end of the frequency range. The greatest value of the square wave analysis lies in the fact that it gives us an entirely different conception of the behavior of an ideal sound system in terms of the unit function. The frequency response characteristic is ordinarily interpreted on the theory that any transient, such as an interval of conversation, may be represented by a Fourier series of sinusoidal frequencies of constant intensity lasting over the entire interval. If these equivalent component frequencies are to be reproduced in their true proportions, the ideal sound system must have mathematically uniform response for all single frequencies. On the other hand, the indicial response characteristic is judged from the Carson extension theorem, which shows that the more closely this characteristic approaches the unit function, the more perfect will be the reproduction of any given transient. Thus, the unit function and the sinusoid may be used as mutually complementary tools of analysis to show different aspects of the same type of problem.

In sound systems which are not ideal, due to inherent physical limitations, we tend to apply the Fourier Theorem out to a certain frequency, just as if it were an ideal system out to this frequency, and then beyond this frequency we do not attempt to sustain the higher frequencies. For most faithful reproduction of transients, it would seem that such practices might be altered somewhat to advantage by allowing the frequency response to drop off more gradually wherever it seems feasible to do so. The exact shape of the ideal curve under these circumstances is a matter of compromise between excessive delay on the one hand and excessive oscillations on the other. In practice, however, a fairly good picture is soon formed when curves such as the last in Figs. 6, 8, and 9 are found to approach the ideal more closely than those of other forms. Such listening tests as have been made tend to confirm these views, but cannot be regarded as being more than an indication.

Square wave analysis is somewhat limited in its practical applications to cases which may be interpreted by inspection. Systems having only a single cutoff frequency, or in the case of an additional low-end cutoff, ratios of the upper and lower cutoff frequencies  $f_2/f_1$  of 100 or more, seem necessary to interpret the results by inspection.

The use of indicial response is not necessarily limited to any particular coupler or method of response measurement, since frequency response and indicial response are so closely related that one is a function of the other. The choice of a closed coupler measurement does, however, permit some interpretation of the results to be made by inspection, whereas other types of measurement may require laborious mathematical means to obtain an interpretation. Other types of vibration instruments, such as recorders, vibration pickups, crystal phonograph reproducers and carbon transmitters, which sustain their response down to zero frequency, should lend themselves to such methods of analysis.

In conclusion, the writer wishes to acknowledge the assistance of Mr. T. J. Pope in connection with the oscillographic work of this paper, and to express his sincere appreciation.

## BIBLIOGRAPHY

1. Oliver Heaviside, "Electromagnetic Theory."
2. J. R. Carson:
  - a. "Transient Oscillations of Electrical Networks and Transmission Systems," *Trans. AIEE*, 1919, p. 445.
  - b. "Electric Circuit Theory and the Operational Calculus," McGraw-Hill.
- 3a. Gilbert Swift, "Amplifier Testing by Means of Square Waves," *Communications*, Vol. 19, No. 2, Feb. 1939.
- 3b. Bedford and Frehendahle, "Transient Response of Multi-Stage Video Frequency Amplifiers," *Proc. I. R. E.*, Vol. 25, No. 4, April 1939.
4. H. E. Kallman, "Portable Equipment for Observing Transient Response of Television Apparatus," *I. R. E. Proc.*, Vol. 28, No. 8, August 1940.
5. L. B. Arguimbau, "Network Testing with Square Waves," *General Radio Experimenter*, Vol. XIV, No. 7, Dec. 1939.
6. W. C. Jones, "Instruments for the New Telephone Sets," *B. S. T. J.* Vol. XVII, No. 3, p. 338, July 1938.
7. V. Bush, "Operational Circuit Theory," Wiley and Sons, p. 176.
8. F. F. Romanow, "Methods for Measuring the Performance of Hearing Aids," *Acous. Soc. Am. Jour.*, Vol. 13, p. 294, Jan., 1942.
9. A. M. Curtis, "A Oscillograph for Ten Thousand Cycles," *B. S. T. J.*, Vol. XII, No. 1, January 1933.

## CHAPTER VII

### Theoretical Analysis of Modes of Vibration for Isotropic Rectangular Plates Having All Surfaces Free

By H. J. McSKIMIN

#### 7.1. INTRODUCTION

The comparatively recent advent of crystal controlled oscillators and of wave filters employing piezoelectric elements has resulted in an extensive study of the ways in which plates made of elastic materials such as quartz or rochelle salt can vibrate. Of special interest have been the resonant frequencies associated with these modes of motion. As will be indicated in subsequent paragraphs, the general solution to the problem of greatest interest is quite complex, and has not been forthcoming, (i.e., as applied to rectangular plates completely unrestrained at all boundary surfaces). For this reason numerous approximate solutions have been developed which yield useful information in spite of their limitations. Several of these solutions will be discussed in the following sections. The three general types of modes (i.e., the extensional, shear, and flexural) will be analyzed in some detail. Also, as a preliminary step the formulation of the general problem along classical lines will be developed.

For the most part, the solutions obtained here are limited to those for an isotropic body. However, such solutions provide considerable guidance for the modes of motion existing in an aeolotropic body such as quartz.

#### 7.2. METHOD OF ANALYSIS

In order to set up the desired mathematical statement of our problem it will be necessary to consider first of all two very fundamental relationships. The first of these is the well known law of Newton which states that a force  $f$  acting on a mass  $m$  produces an acceleration  $a$  in accordance with the formula

$$f = m \cdot a$$

The second relationship which we shall need is Hooke's law relating the strains in a body to the stresses. If forces are applied to the ends of a long slender rod made of an elastic material such as steel (Fig. 7.1) a certain amount of stretching takes place. If the forces are not too great, a linear

relationship between the applied stress and ensuing strain is found to exist. Expressed as an equation

$$\frac{X_x}{x_x} = E \quad \text{in which } X_x \text{ is the force per unit area,}$$

$x_x$  is the strain per unit length, and  $E$  is a constant known as Young's Modulus. (Refer to Section 7.7 for further definition of terms).

In an analogous manner, shearing stresses applied to an elastic solid as shown by Fig. 7.2 produce a shearing strain such that

$$\frac{X_y}{x_y} = A, \quad \text{the shear modulus.}$$

In general there will be contributions to a particular strain from any of the stresses which may happen to exist. For example, when an isotropic

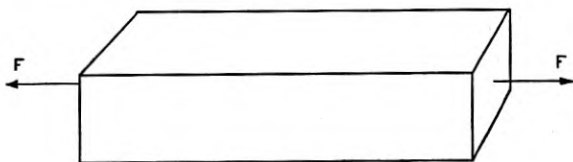


Fig. 7.1—Bar under tensional stress

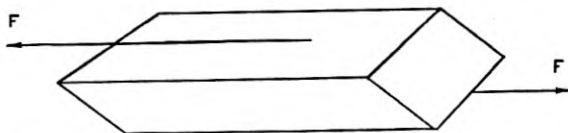


Fig. 7.2—Bar under shearing stress

bar is stretched, there will be a contraction along the width which has been produced by a stress along the length. A statement of these relationships (known as Hooke's Law) is given by the equations of Section 7.8.

It is now of interest to consider the conditions of equilibrium for a very small cube cut out of the elastic medium which in general is stressed and in motion. Reference to Fig. 7.3 will help to visualize the stresses which may exist on the faces of this cube. Since these stresses vary continuously within the medium, a summation of the forces acting on the cube along each of the major axes can be made with the use of differential calculus. From Newton's Law previously cited, it is apparent that any unbalance of these forces will result in an acceleration inversely proportional to the mass of our small cube. Three equations may then be derived, one for each major direction.<sup>1</sup> If only simple harmonic motion is considered (i.e. all displace-

<sup>1</sup> Refer to "Theory of Elasticity" by S. Timoshenko or to any standard text on elasticity.

ments are proportional to  $\sin \omega t$  where  $\omega = 2\pi$  times frequency) the following simplified equations result.

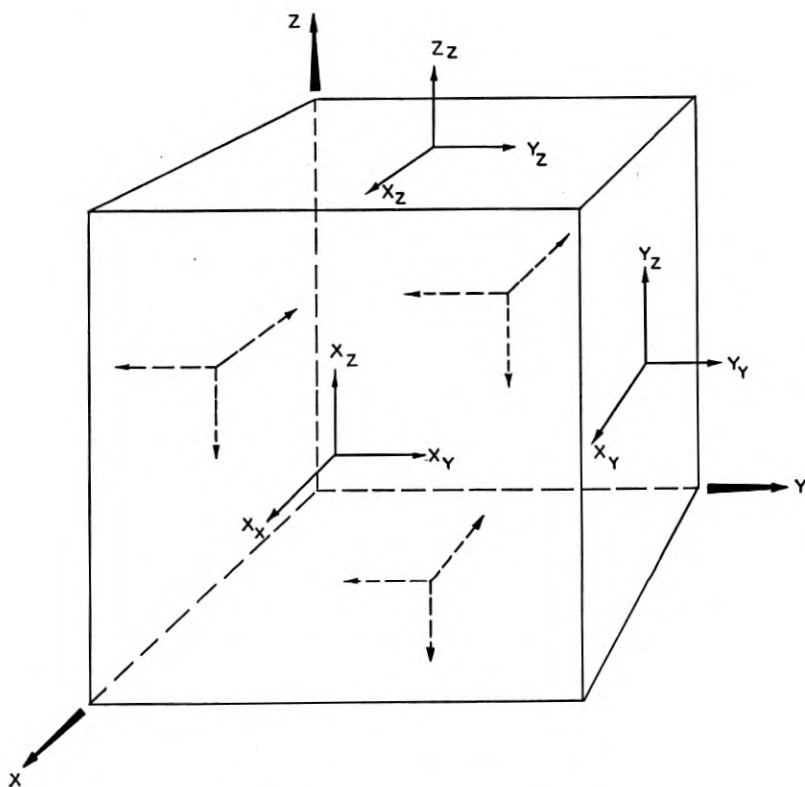


Fig. 7.3—Stresses acting on small cube.

$$\left. \begin{aligned} \frac{\partial X_x}{\partial x} + \frac{\partial X_y}{\partial y} + \frac{\partial X_z}{\partial z} &= -\rho\omega^2 u \\ \frac{\partial Y_y}{\partial y} + \frac{\partial X_y}{\partial x} + \frac{\partial Y_z}{\partial z} &= -\rho\omega^2 v \\ \frac{\partial Z_z}{\partial z} + \frac{\partial X_z}{\partial x} + \frac{\partial Y_z}{\partial y} &= -\rho\omega^2 w \end{aligned} \right\} \quad (7.1)$$

Since stresses are related to strains in a very definite manner, the above equations may be converted into a more useful form involving only displacements. For *isotropic media*, the following results.

$$\left. \begin{aligned} A\nabla^2 u + B \frac{\partial \epsilon}{\partial x} &= -\rho\omega^2 u \\ A\nabla^2 v + B \frac{\partial \epsilon}{\partial y} &= -\rho\omega^2 v \\ A\nabla^2 w + B \frac{\partial \epsilon}{\partial z} &= -\rho\omega^2 w \end{aligned} \right\} \quad (7.2)$$

In this grouping,

$$\begin{aligned} \nabla^2 &= \frac{\partial^2}{\partial x^2} + \frac{\partial^2}{\partial y^2} + \frac{\partial^2}{\partial z^2} \\ \epsilon &= \frac{\partial u}{\partial x} + \frac{\partial v}{\partial y} + \frac{\partial w}{\partial z} \end{aligned}$$

and  $A$  and  $B$  are given in terms of the fundamental elastic constants  $\lambda$  and  $\mu$  with  $A = \mu$ ,  $B = \lambda + \mu$ .

An even more elegant statement of the equilibrium conditions attributable to Love<sup>2</sup> follows immediately from equations 7.2, since by differentiating each one in turn with respect to  $x$ ,  $y$ , and  $z$  respectively, and then adding results, one obtains the wave equation

$$(\nabla^2 + h^2)\epsilon = 0 \quad (7.3)$$

where

$$h^2 = \frac{\rho\omega^2}{A + B} = \frac{\rho\omega^2}{\lambda + 2\mu}$$

Whatever our solution may be, then, it must satisfy equation (7.3). If such an expression for  $\epsilon$  is found, the displacements formed in the following way will satisfy equations 7.2 as can be shown by direct substitution.

$$u = -\frac{1}{h^2} \frac{\partial \epsilon}{\partial x} \quad v = -\frac{1}{h^2} \frac{\partial \epsilon}{\partial y} \quad w = -\frac{1}{h^2} \frac{\partial \epsilon}{\partial z} \quad (7.4)$$

In addition to equations 7.2, another set of requirements will be necessary when any particular problem is considered. They are known as the boundary conditions, and in general are easily deduced from a knowledge of how the plate or bar is held.

For a rectangular plate free on all surfaces, the boundary condition is simply that all surface tractions vanish. This requires certain stresses to become zero at the boundary as can be seen from the following expressions for the  $x$ ,  $y$ , and  $z$  components of traction in terms of unit stresses.

<sup>2</sup> A. E. Love, "A Treatise on the Mathematical Theory of Elasticity."

$$\left. \begin{aligned} \bar{X} &= X_x \ell + X_y m + X_z n \\ \bar{Y} &= Y_x m + Y_y n + X_y \ell \\ \bar{Z} &= Z_x n + X_z \ell + Y_z m \end{aligned} \right\} = 0 \text{ for free surfaces} \quad (7.5)$$

( $\ell$ ,  $m$ , and  $n$  are direction cosines of the normal to the surface at the point in question).

The general problem is now seen to be one of finding solutions for the displacements  $u$ ,  $v$ , and  $w$  such that both the equilibrium and boundary conditions are satisfied. In the following section several interesting solutions will be considered for rectangular plates having all surfaces free, this being the case of greatest interest in so far as this paper will be concerned.

### 7.3. EXTENSIONAL VIBRATIONS

One of the most useful modes of vibration of practical interest is the extensional, in which particle motion takes place in essentially one direction so as to alternately stretch and compress the elastic medium. Piezoelectric

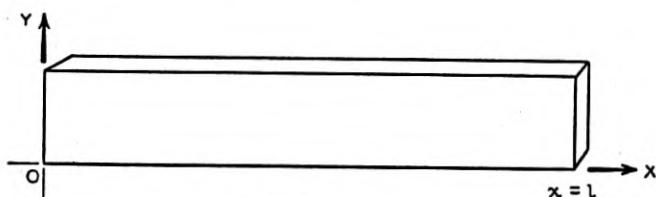


Fig. 7.4—Longitudinal bar

plates vibrating in this manner, and of the shapes shown in figures 7.4 and 7.5 have been used extensively in wave filter and oscillator circuits. The approximate resonant frequencies corresponding to this type of motion are easily obtained by a consideration of equations 7.1 and 7.2. For the longitudinal bar of Fig. 7.4 the only stress that need be considered is the  $X_x$  extensional, all other stresses being so small that they can be neglected. The equilibrium equation then becomes

$$\frac{\partial X_x}{\partial x} = -\rho \omega^2 u \quad (7.6)$$

or, since

$$\begin{aligned} \frac{\partial u}{\partial x} &= \frac{1}{E} X_x \\ \frac{\partial^2 u}{\partial x^2} &= -\frac{\rho}{E} \omega^2 u \end{aligned} \quad (7.7)$$

It is easily seen that  $u = \cos kx$  is a solution to this equation if  $k = \omega \sqrt{\frac{\rho}{E}}$ . If now the boundary condition that the stress  $X_x$  must become zero at the ends of the bar (i.e.,  $x = 0, x = \ell$  — refer to Eq. (7.5)), is fulfilled, the solution will be complete. At  $x = 0, X_x = E \frac{\partial u}{\partial x}$  will always equal zero. Furthermore, if  $k = \frac{\pi}{\ell}$  or any whole number multiple of  $\frac{\pi}{\ell}$  the extensional stress will likewise reduce to zero at  $x = \ell$ . The desired solution will then be as follows,  $f$  being the resonant frequencies.

$$\left. \begin{aligned} u &= \cos \omega \sqrt{\frac{\rho}{E}} x \\ \omega &= 2\pi f = \frac{m\pi}{\ell} \sqrt{\frac{E}{\rho}} \\ m &= 1, 2, 3, \text{ etc.} \end{aligned} \right\} \quad (7.8)$$

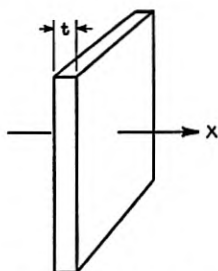


Fig. 7.5—Thin plate

The plate of Fig. 7.5 will now be considered. Here it can no longer be assumed that the  $X_x$  stress is the only one of importance. Instead, the displacements  $v$  and  $w$  will be considered zero and the displacement  $u$  a function of  $x$  only. This means that the shear stresses  $X_y, X_z, Y_x$  vanish, so that the equilibrium equations 7.2 reduce to

$$A \frac{\partial^2 u}{\partial x^2} + B \frac{\partial^2 u}{\partial x^2} = -\rho \omega^2 u \quad (7.9)$$

or

$$\frac{\partial^2 u}{\partial x^2} = \frac{-\rho \omega^2 u}{A + B} \quad (7.10)$$

This is seen to be of the same form as equation (7.7) previously discussed, and will again have the solution  $u = \cos kx$  with  $k = \omega \sqrt{\frac{\rho}{A + B}}$ . The

boundary condition on the  $X_x$  stress will be met if  $k = \frac{m\pi}{t}$  so that the following solutions result.<sup>3</sup>

$$\begin{aligned}
 u &= \cos \omega \sqrt{\frac{\rho(1 + \sigma)(1 - 2\sigma)}{E(1 - \sigma)}} x = \cos \omega \sqrt{\frac{\rho}{\lambda + 2\mu}} x \\
 \omega &= 2\pi f = \frac{m\pi}{t} \sqrt{\frac{E}{\rho} \frac{(1 - \sigma)}{(1 + \sigma)(1 - 2\sigma)}} = \frac{m\pi}{t} \sqrt{\frac{\lambda + 2\mu}{\rho}} \quad (7.11) \\
 m &= 1, 2, 3, \text{ etc.}
 \end{aligned}$$

It is seen that this formula for resonant frequencies is the same as given by equations 7.8, with  $E$  replaced by  $\frac{E \cdot (1 - \sigma)}{(1 - 2\sigma^2 - \sigma)}$ , so that the frequency constant  $f \cdot t$  will be somewhat higher than  $f \cdot \ell$  for a long slender bar.

It is recognized that the solutions derived above hold true only for the limiting cases of a long slender bar, and a very thin plate respectively. It is therefore of interest to trace the resonant frequencies corresponding to these extensional modes of vibration as departure is made from the limiting cases mentioned above.

An experimental plot of the resonant frequencies of a thin plate of length  $\ell$  and width  $w$  reveals that the frequency of the longitudinal mode first discussed is gradually lowered as the width of the plate is increased. There is also another frequency corresponding to an extensional vibration along the width which for a very narrow plate corresponds to the second type of extensional mode considered in the foregoing paragraphs, except that the frequency constant will be slightly different because coplanar stresses are involved.

As seen from Fig. 7.6, the resonant frequency curves do not cross, but exhibit coupling effects. This is understandable from the fact that motion in one direction is mechanically coupled to motion in the other as indicated by Poisson's ratio  $\sigma$ .

In order to derive expressions for the  $u$  and  $v$  displacements associated with the extensional mode along the length, taking into account the above coupling effect, the following analysis proves interesting.

Consider the infinite isotropic strip of width  $b$  as shown by figure 7.7. As will be demonstrated presently, solutions can be found such that the equilibrium equations and the boundary conditions are precisely satisfied. Furthermore it will be found possible to cut a section out of this strip in

<sup>3</sup> If the length and width of the plate are very large in comparison to the thickness, the boundary conditions for the  $Y_y$  and  $Z_z$  stresses may be neglected without causing appreciable error. The quantity  $A + B$  has been evaluated in terms of  $E$  and  $\sigma$  for purposes of comparison.

such a way that the boundary conditions for the cut edges are very nearly satisfied. The plate formed in this way may then be considered as vibrating at the required frequency  $f$ , which will then be the resonant frequency desired.

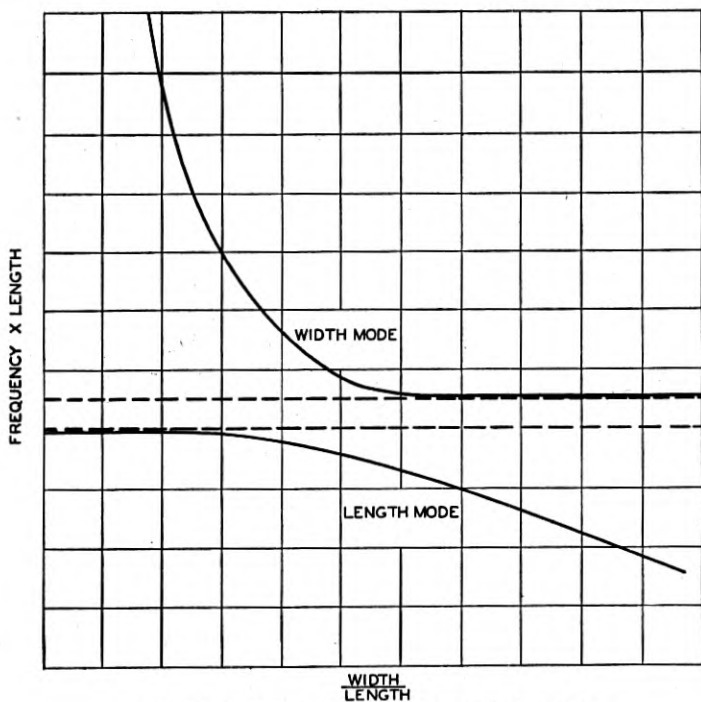


Fig. 7.6—Extensional modes with mechanical coupling

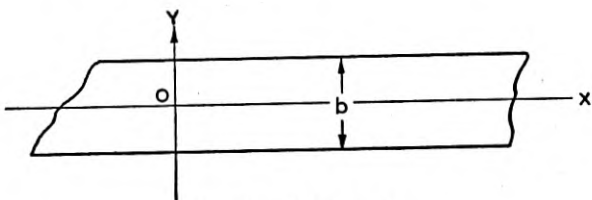


Fig. 7.7—Infinite strip

Let displacements be arbitrarily chosen in the following way:

$$\left. \begin{aligned} u &= U \cos kx \cos \ell_y \\ v &= V \sin kx \sin \ell_y \end{aligned} \right\} \quad (7.12)$$

As shown in Section 7.9, two solutions of this type will satisfy the equilibrium equations precisely. One corresponds to  $\epsilon = 0$  in the wave equation 7.3, while for the other  $\epsilon \neq 0$ . Superposition of these two solutions and proper evaluation of parameters make it possible to satisfy the boundary conditions at the edge of the strip; namely, that at  $y = \pm \frac{b}{2}$ ,  $Y_v = 0$  and  $X_v = 0$ . (Refer to equations 7.5). The following transcendental equation is obtained

$$\frac{\cot \ell_1 \frac{b}{2}}{\cot \ell_2 \frac{b}{2}} = \frac{-2\ell_1 \ell_2 k^2 (1 - \sigma)}{(\ell_2^2 - k^2)(\ell_1^2 + \sigma k^2)} \quad (7.13)$$

in which

$$\left. \begin{aligned} \ell_1^2 &= \frac{A}{A+B} \theta^2 - k^2 \\ \ell_2^2 &= \theta^2 - k^2 \\ \theta^2 &= \frac{\rho \omega^2}{A} \end{aligned} \right\} \quad (7.14)$$

This equation may be solved graphically to yield values of frequency corresponding to given values of  $k$ . For our discussion of the length extensional mode of vibration, the first root only will be considered.

Fig. 7.8 shows a plot of  $\theta \cdot b$  against  $b \cdot k$  assuming that Poisson's ratio is .33.<sup>4</sup> If  $k = 1$ , and  $b = 1$ , for example,  $\theta = \sqrt{\frac{\rho}{A}} \omega = 1.62$ .

The equations for the displacements when determined as explained in Section 7.9 become:

$$\begin{aligned} u &= U_1 [\cosh .344 y + .402 \cos 1.278 y] \cos x \\ v &= U_1 [.344 \sinh .344 y + .315 \sin 1.278 y] \sin x \end{aligned} \quad (7.15)$$

All three stresses  $X_x$ ,  $Y_v$ , and  $X_v$  may be calculated from the above equations. If the length of our plate is made equal to  $m\pi$ , where  $m$  is an integer, the extensional stress  $X_x$  will equal zero regardless of  $y$  at the boundaries  $x = 0$  and  $x = \ell$  since  $X_x \propto \sin x = 0$  when  $x = m\pi$ . Also it can be shown by calculation that  $X_v$  is so small in comparison to the extensional stresses as to be entirely negligible; hence our solution is complete.

If  $\ell = \pi$ , the plate will be vibrating in its fundamental longitudinal mode. The distortion which results is shown by Fig. 7.9. It is seen that most of

<sup>4</sup> Plotted in this way, the same curve results regardless of the value of  $b$  chosen for the purpose of solving Eq. 7.13.

the motion is along the  $x$  axis, though there is a certain amount of lateral contraction as the plate elongates.

The second harmonic will have the same resonant frequency if  $\ell = 2\pi$ , the third if  $\ell = 3\pi$ , etc.

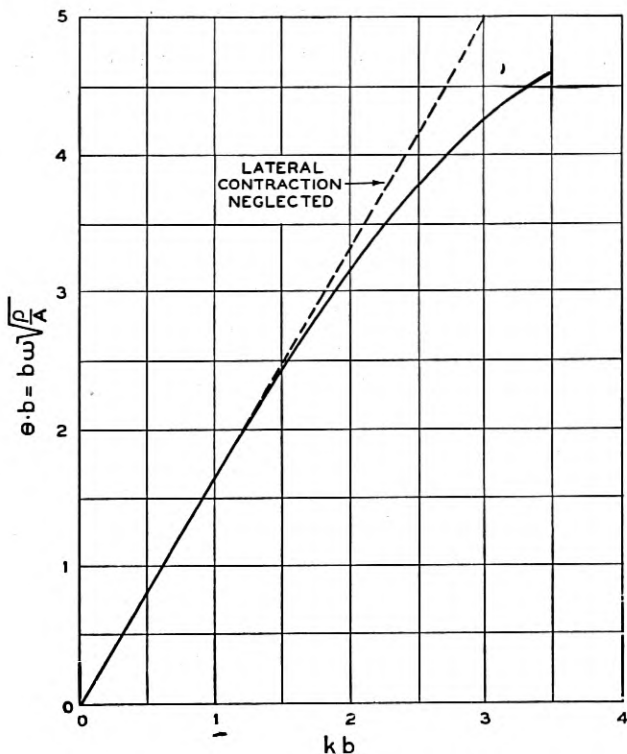


Fig. 7.8— $\theta \cdot b$  versus  $k \cdot b$  for plate longitudinal modes ( $\sigma = .33$ ,  $k = \frac{m\pi}{\text{length}}$ )

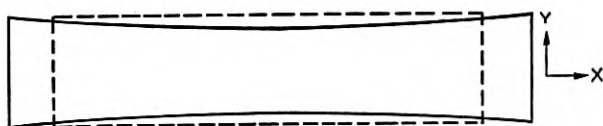


Fig. 7.9—Distortion of plate vibrating in first longitudinal mode

In addition to harmonic modes along the length just considered there will be those for which the motion breaks up along the width. In general, the distortion of the plate may be quite complex with simultaneous variations along both dimensions. Similarly, for plates such as shown in Fig. 7.5

there will be many extensional modes which have resonant frequencies somewhat above those given by Eq. 7.11. Analysis of the motion shows that for these modes the displacement along the thickness varies periodically (or "breaks up") along the major dimensions of the plate. There again the distortion pattern of the plate may become very complex.

#### 7.4. SHEAR VIBRATIONS

The second class of vibrations which will now be considered is the shear. This type of mode is of special importance because of the fact that piezoelectric plates vibrating in shear are widely used for frequency control of oscillators. For example, the AT quartz plate which is so much in demand utilizes a fundamental thickness shear mode in which particle motion is principally at right angles to the thickness. The distortion of the plate will be similar to that shown in Fig. 7.2.

A simple, yet very useful formula for the resonant frequencies associated with the above type of displacement has been derived on the assumption

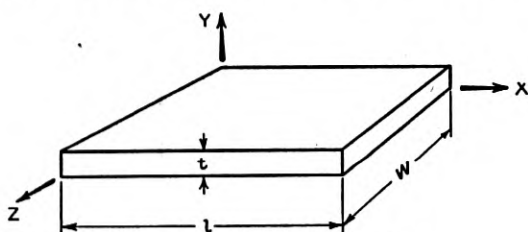


Fig. 7.10—Orientation of thin plate

that the length and width of the plate are very large in comparison to the thickness. For the  $xy$  shear mode, the displacement  $u$  is assumed to be  $u = U \cos ky$ , all other displacements being equal to zero. The only stress that need be considered then, is the  $X_y$  shear which is proportional to  $\sin ky$ . Boundary conditions on this stress at the major surfaces of the plate are easily satisfied by choosing  $k$  such that  $X_y = 0$  at  $y = 0$  and  $y = t$ . (Refer to Fig. 7.10.) This will be the case if  $k = \frac{m\pi}{t}$ , where  $m$  is any integer, and  $t$  is the thickness of the plate. By using the simplified equilibrium equation as reduced from equations 7.1, a formula for the resonant frequencies is obtained in much the same manner as for extensional thickness modes.

$$\omega = 2\pi f = \frac{m\pi}{t} \sqrt{\frac{A}{\rho}} \quad m = 1, 2, 3, \text{ etc.} \quad (7.16)$$

In this formula the shear modulus  $A$  appears instead of Young's modulus as in the case of longitudinal modes. Harmonic modes are given by values of  $m$  greater than unity.

In addition to the resonant frequencies predicted by the foregoing analysis, there will be others corresponding to shear vibrations in which the principal shear stress varies periodically along the length and width of the plate. A formula which yields the approximate frequencies for these modes is developed in Section 7.9. It is shown that if the length and width are large in comparison to the thickness, the following expression may be used:

$$\omega = 2\pi f = \pi \sqrt{\frac{1}{\rho}} \sqrt{c_{11} \frac{n^2}{\ell^2} + \frac{c_{66} m^2}{\ell^2} + \frac{c_{55} p^2}{w^2}} \quad (7.17)$$

In this formula which has been derived for  $xy$  shears the  $c$  constants are the standard elastic constants for aeolotropic media. For isotropic plates such as have been considered up to this point

$$c_{11} = \frac{E(1 - \sigma)}{1 - 2\sigma^2 - \sigma} = \lambda + 2\mu$$

and

$$c_{55} = c_{66} = A, \text{ the shear modulus} \quad (7.18)$$

Various combinations of the integers  $m$ ,  $n$ , and  $p$  may be chosen, with the restriction that neither  $m$  nor  $n$  can equal zero. It is seen that if  $\ell$  and  $w$  are very large the formula reduces to that of Eq. 7.16 which was derived on precisely that basis. Also, it is seen that the more complex modes all lie somewhat above the fundamental shear obtained by setting  $m = n = 1$  and  $p = 0$ .

Plate shear modes are also of considerable interest, particularly the one of lowest order. For a plate having a large ratio of length to width a formula similar to that given by equation 7.17 (but for two dimensions only) may be developed. If the plate is nearly square, however, this formula no longer yields sufficiently accurate values for the resonant frequencies. Coupling to other modes of motion<sup>5</sup> complicates the problem so much that only experimental results have been of much practical consequence. Fig. 7.11 shows in an exaggerated way the distortion of a nearly square plate vibrating in the first shear mode.

## 7.5. FLEXURAL VIBRATIONS

### 7.51. Plate Flexures

One of the most studied types of vibrations has been the flexural. Perhaps this is true because it is the most apparent and comes within the realm of experience of nearly everyone. The phenomena of vibrating reeds, xylophone bars, door bell chimes, tuning forks, etc. are quite well known.

<sup>5</sup> It is found experimentally that odd order shears are strongly coupled to even order flexures; similarly, even order shears and odd order flexures are coupled.

Beam theory has been used quite extensively to derive the equations which yield the resonant frequencies and displacements for bars vibrating in flexure. To obtain reasonably accurate results for ratios of width to length approaching unity, however, the effects of lateral contraction, rotary inertia, and shearing forces must be considered. This leads to a rather complicated solution which is much more accurate than that derived by the use of simple beam theory only, though it is still approximate in nature.

For two dimensional plates free on all edges a method of analysis may be used which is similar to that described under extensional modes. While it is somewhat involved it yields direct expressions for the two displacements  $u$  and  $v$ , so that all stresses may be calculated, and the extent to which boundary conditions are satisfied determined.<sup>6</sup>

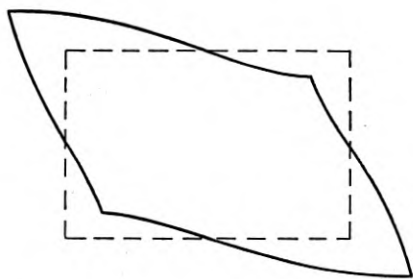


Fig. 7.11—Distortion of plate in first shear mode

Solutions for  $u$  and  $v$  are assumed to be of the form

$$\begin{aligned} u &= U \sin \ell y \cos kx \\ v &= V \cos \ell y \sin kx \end{aligned} \quad (7.19)$$

For the infinite strip previously considered a transcendental equation is obtained which is the same as equation 7.13 with the exception that the left-hand expression is inverted.

$$\frac{\tan \ell_1 \frac{b}{2}}{\tan \ell_2 \frac{b}{2}} = \frac{-2\ell_1 \ell_2 k^2 (1 - \sigma)}{(\ell_2^2 - k^2)(\ell_1^2 + \sigma k^2)} \quad (7.20)$$

(Refer to Eq. 7.14 also.)

<sup>6</sup> This is an extension of Doerffler's analysis used to obtain harmonic flexure frequencies for plates—"Bent and Transverse Oscillations of Piezo-Electrically Excited Quartz Plates"—*Zeitschrift Für Physik*, v. 63, July 7, 1930, p. 30. Also refer to "The Distribution of Stress and Strain for Rectangular Isotropic Plates Vibrating in Normal Modes of Flexures"—New York Univ. Thesis by Author, June 1940.

The lowest order solution to this equation is found to correspond to flexure vibrations in the infinite strip. A calculation of stresses, however, reveals that boundary conditions cannot be satisfied properly even for the case of a long narrow plate. It can be shown, however, that another solution may be derived for the same value of frequency by letting  $k$  become imaginary. This simply means that the  $u$  and  $v$  displacements become hyperbolic functions of  $x$  instead of sinusoidal. The two complete solutions for the infinite strip may then be superimposed and parameters adjusted so that for definite values of length corresponding to fundamental and harmonic modes the proper stresses reduce essentially to zero on the ends of the plate. For plates having a ratio of width to length less than .5, this method gives very accurate expressions for displacements and stresses. If only the resonant frequency is required, ratios up to unity and beyond (for the fundamental mode) may be considered.

An example has been worked out to provide a complete picture of the displacements for a bar of width = 1,  $k = 1$  and  $\sigma = .33$ . Use of equation 7.20 yields the quantity  $\theta^2 = \frac{\rho\omega^2}{A} = .166$  from which the resonant frequency may be obtained. Using this value of  $\theta^2$ , one finds that  $k^2 = -.800$  also satisfies equation 7.20. By making the total length of the bar equal to 4.50 the  $X_x$  extensional stress and the  $X_y$  shear stress may be made essentially zero on the ends of the plate regardless of  $y$ .<sup>7</sup>

The following expressions for  $u$  and  $v$  are obtained:

$$\begin{aligned} u &= (\sinh .9132 y - 1.02 \sinh .9718y) \sin x \\ &\quad - .160 (\sin .9828y - .9568 \sin .9250y) \sinh .8944x \\ v &= (-1.094 \cosh .9132y + .9915 \cosh .9718) \cos x \\ &\quad - .160 (.9095 \cos .9828y - .990 \cos .9250y) \cosh .8944x \end{aligned} \quad (7.21)$$

Fig. 7.12 shows the distortion of the plate as calculated from the above expressions. It is seen that there will be two points at which there is no motion in either the  $x$  or  $y$  directions. These nodal points can be used in holding the plate, since it may be clamped firmly there without altering the displacements or resonant frequency. For the example shown, these nodes are positioned a distance of  $.211\ell$  from the ends of the plate as compared to  $.224\ell$  for a long thin bar.

<sup>7</sup> A graphical solution to determine  $\ell$  is most convenient in which parameters are adjusted so that  $X_x = 0$  at  $x = \pm \frac{\ell}{2}$  and  $y = \pm \frac{b}{2}$ ;  $X_y = 0$  at  $x = \pm \frac{\ell}{2}$  and  $y = 0$ . These stresses will remain essentially zero for all values of  $y$  if the ratio of  $\frac{w}{\ell}$  is not too great.

Figures 7.13 and 7.14 show the distribution of the principle stresses as a function of position along the length. It is seen that for the particular

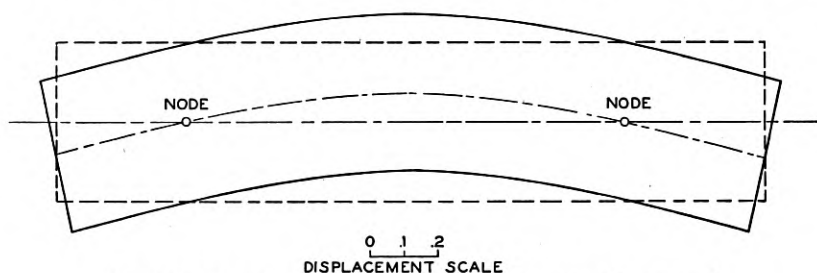


Fig. 7.12—Distortion of bar vibrating in first free-free flexure mode

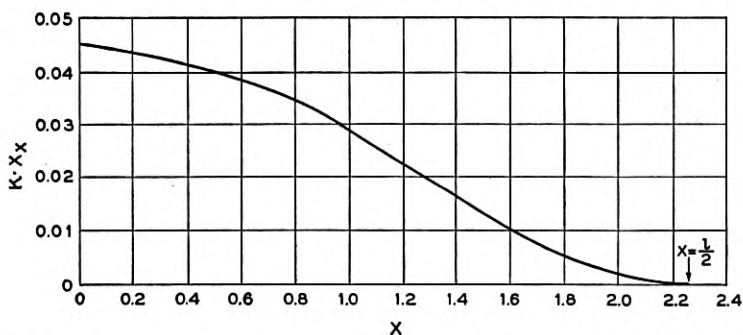


Fig. 7.13—Distribution of longitudinal stress for free-free bar vibrating in first flexure mode

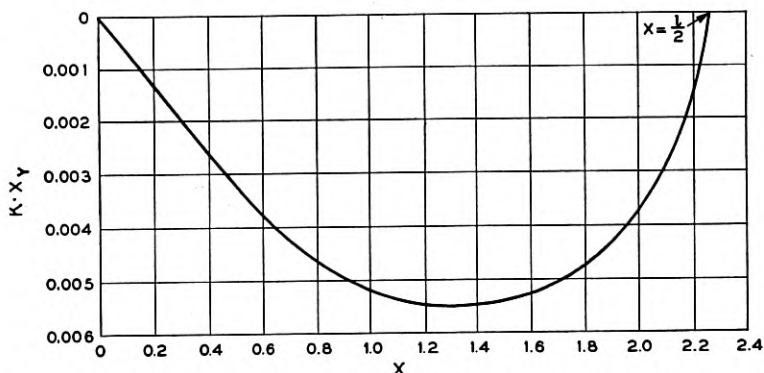


Fig. 7.14—Distribution of shear stress for free-free bar vibrating in first flexure mode

example cited, the maximum shear stress is only about one-tenth the maximum  $X_x$  extensional stress. Both of these stresses reduce to zero at

the ends of the plate as they should in order to satisfy the boundary conditions. As the ratio of  $\frac{w}{l}$  is increased the shear stress becomes of greater importance.

### 7.52. Thickness Flexures

The final analysis to be considered in this paper is for thickness flexures along the width or length of a thin plate. These modes are of particular interest in connection with the dimensioning of quartz plates for which it is desirable to utilize the fundamental thickness shear mode. (AT plate, for example.) It is found experimentally that even ordered thickness flexures are coupled to this shear to such a degree that at certain ratios of dimensions the operation of the plate as an oscillator or filter component is impaired.

The two-dimensional solution derived in the preceding paragraphs can be used to predict certain harmonic thickness flexures; however, in order to obtain a complete picture it is necessary to extend the theory to three dimensions. This has been done by the author with the following transcendental equation as a result (refer to Section 7.93).

$$\frac{\tan \ell_1 \frac{b}{2}}{\tan \ell_2 \frac{b}{2}} = \frac{-2\ell_1 \ell_2 A \alpha^2}{[\sigma B(\ell_1^2 + \alpha^2) + A\ell_1^2][\ell_2^2 - \alpha^2]} \quad (7.22)$$

Solutions to this equation are exact in nature for a plate of thickness  $b$  and of infinite extent in both the  $x$  and  $z$  directions. The quantity  $\alpha^2$  is equal to the sum of the squares of  $k$  and  $m$  which appear in the expressions for displacements as follows:

$$\left. \begin{aligned} u &= U f_1(y) \sin kx \cos mz \\ v &= V f_2(y) \cos kx \cos mz \\ w &= W f_3(y) \cos kx \sin mz \end{aligned} \right\} \quad (7.23)$$

Also in equation (7.22)

$$\left. \begin{aligned} \ell_1^2 &= \theta^2 \frac{A}{A+B} - \alpha^2 \\ \ell_2^2 &= \theta^2 - \alpha^2 \\ \theta^2 &= \frac{\rho \omega^2}{A} \end{aligned} \right\} \quad (7.24)$$

The lowest order solution to equation (7.22) with  $\alpha^2$  positive again corresponds to flexure vibrations, as in the two dimensional case. Fig. 7.15 shows a plot of  $\theta \cdot b$  against  $\alpha \cdot b$  calculated for  $\sigma = .3$ .

For reasonably high order flexures it may be reasoned that the true displacements will be very nearly the same as those for the doubly infinite plate as derived by the above method since the correction necessary to fulfill the boundary conditions will only apply very close to the edges of the plate. It will then be sufficient to choose values for  $k$  and  $m$  such that  $k = p \frac{\pi}{\ell}$  and  $m = \frac{q\pi}{w}$  where  $p$  and  $q$  are integers. The values of  $\alpha^2$  obtained in this way determine the corresponding resonant frequencies.

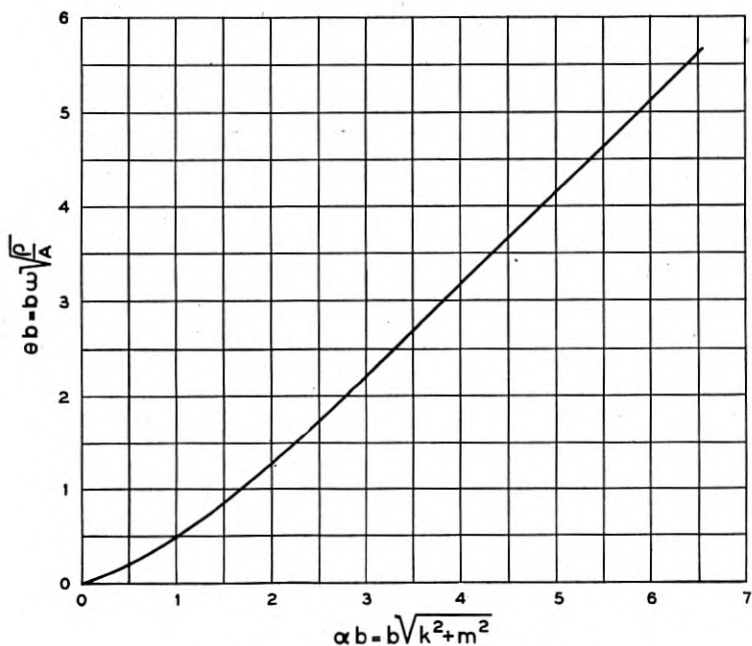


Fig. 7.15— $\theta \cdot b$  versus  $\alpha \cdot b$  for thickness flexures

If it is desired to solve for the ordinal  $xy$  flexures, for example,  $m$  should be set equal to zero. The displacements in this case will be independent of the  $z$  dimension. When  $q$  is assigned values other than zero however, the resulting modes may be considered as  $xy$  flexures which vary or break up along the third major dimension. If  $q$  is small the resonant frequencies will lie only slightly higher than that of the corresponding ordinal flexure for which  $q = 0$ .

Fig. 7.16 shows a few of the resonant frequencies as calculated for values of shear modulus and density corresponding to AT quartz. The effects of coupling to the fundamental thickness shear are shown by dotted lines for the 14th  $xy$  flexure. As might be expected there is similar coupling between

the 14th flexure which breaks up once along the  $z$  dimension and the shear which breaks up once along  $z$ —etc. A few of these flexures which break up along  $z$  are shown for the 16th ordinal flexure.

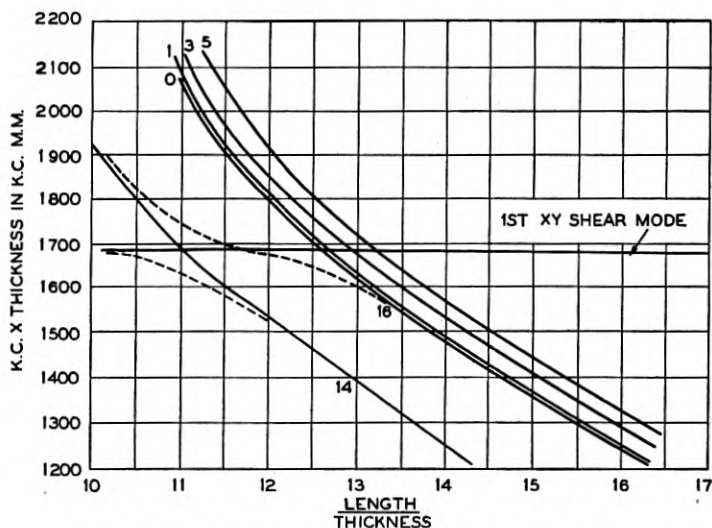


Fig. 7.16—XY thickness flexure modes for square plate

## 7.6. SUMMARY

Three main classes or families of vibrational modes are found to exist in rectangular elastic plates free on all surfaces; namely, the extensional, the shear, and the flexural. In general, the associated displacements are functions of all three dimensions and may vary in such a manner as to make the distortion of such plates quite complex.

For certain limiting cases, approximate solutions for the resonant frequencies and displacements (from which strains and stresses may be calculated) can be derived. Though there are a number of methods that can be used for specific problems, it has been found very convenient to utilize the classical formulation. For this reason the basis of this method has been discussed briefly. In essence it requires that displacements and stresses occurring within the elastic solid satisfy conditions of equilibrium as derived from Newton's Law. At the boundaries, certain other relations must be satisfied in order that conditions of clamping might be fulfilled. For plates entirely unrestrained the latter requires that all forces (tractions) acting through the free surfaces must vanish.

For thin rectangular plates (such as quartz crystal oscillator plates) the modes of greatest practical consequence are plate modes, for which all

stresses are essentially coplanar and independent of the thickness, and thickness modes, for which all dimensions must be considered except in limiting cases.

Because of their great utility, simplified formulae have been derived for the resonant frequencies associated with long, narrow bars vibrating longitudinally, thin plates with extensional motion along the thickness dimension, and thin plates vibrating with shearing motion at right angles to the thickness.

Exact solutions for the infinite strip have been derived, and used in obtaining the displacements and resonant frequencies for flexural and longitudinal modes. Such solutions take account of the fact that the width of the plate may become appreciable. While limiting cases of plate shear may be analyzed, solutions for ratios of  $\frac{w}{t}$  approaching unity have not proved very satisfactory. This is attributable to the fact that coupling to flexural modes is severe.

Thickness flexural modes which exhibit displacement variations along both length and width dimensions of the plate have been analyzed by extending the "infinite strip" theory to three dimensions. Solutions obtained are fairly accurate if the harmonic order of the flexure is sufficiently great.

#### 7.7. NOMENCLATURE

$\rho$  = density

$E$  = Young's modulus

$\sigma$  = Poisson's ratio

$A$  = Shear modulus =  $\frac{E}{2(1 + \sigma)} = \mu$

$B = \frac{E}{2(1 + \sigma)(1 - 2\sigma)} = \lambda + \mu$  for 3 dimensions  
 $= \frac{E}{2(1 - \sigma)}$  for plane stress

$\omega$  = angular velocity =  $2\pi f$

$\theta^2 = \frac{\rho\omega^2}{A}$

$u, v, w$  = displacements in  $x, y$  and  $z$  directions

$\epsilon = \frac{\partial u}{\partial x} + \frac{\partial v}{\partial y} + \frac{\partial w}{\partial z}$

$$\nabla^2 = \text{Laplacian} = \frac{\partial^2}{\partial x^2} + \frac{\partial^2}{\partial y^2} + \frac{\partial^2}{\partial z^2}$$

$\left. \begin{matrix} x_x, y_y, z_z \\ x_y, x_z, y_z \end{matrix} \right\}$  unit strain components

$\left. \begin{matrix} X_x, Y_y, Z_z \\ X_y, X_z, Y_z \end{matrix} \right\}$  unit stresses

### 7.8. STRESS-STRAIN EQUATIONS FOR ISOTROPIC MEDIA

$$x_x = \frac{1}{E} (X_x - \sigma Y_y - \sigma Z_z)$$

$$y_y = \frac{1}{E} (Y_y - \sigma X_x - \sigma Z_z)$$

$$z_z = \frac{1}{E} (Z_z - \sigma X_x - \sigma Y_y)$$

$$\text{shear strain} = \frac{1}{A} \times \text{shear stress}$$

$$X_x = 2 \left( \sigma B \epsilon + A \frac{\partial u}{\partial x} \right)$$

$$Y_y = 2 \left( \sigma B \epsilon + A \frac{\partial v}{\partial y} \right)$$

$$Z_z = 2 \left( \sigma B \epsilon + A \frac{\partial w}{\partial z} \right)$$

$$X_y = A \left( \frac{\partial u}{\partial y} + \frac{\partial v}{\partial x} \right)$$

$$X_z = A \left( \frac{\partial u}{\partial z} + \frac{\partial w}{\partial x} \right)$$

$$Y_z = A \left( \frac{\partial v}{\partial z} + \frac{\partial w}{\partial y} \right)$$

For plane stress in  $xy$  plane

$$x_x = \frac{1}{E} (X_x - \sigma Y_y)$$

$$y_y = \frac{1}{E} (Y_y - \sigma X_x)$$

$$x_y = \frac{1}{A} X_y$$

$$X_x = \frac{E}{1 - \sigma^2} (x_x + \sigma y_y)$$

$$Y_y = \frac{E}{1 - \sigma^2} (y_y + \sigma x_x)$$

$$X_y = A x_y$$

7.9. MATHEMATICAL DERIVATIONS

7.91. Longitudinal Vibrations in Two-Dimensional Plates

As explained in the text, solutions for the infinite strip of Fig. 7.7 are first derived. Let

$$\left. \begin{aligned} u &= U \cos kx \cos \ell_y \\ v &= V \sin kx \sin \ell_y \end{aligned} \right\} \quad (7.12)$$

where  $U$  and  $V$  are constant. From these expressions  $\epsilon = \frac{\partial u}{\partial x} + \frac{\partial v}{\partial y}$  can

be obtained and substituted into the equilibrium equations 7.2. Two expressions as follows result after dividing through by the common term  $\cos kx \cos \ell_y$ .

$$A(k^2 + \ell^2) - \frac{Bk}{U} (-kU + \ell V) = \rho\omega^2 \quad (7.25)$$

$$A(k^2 + \ell^2) + \frac{B\ell}{V} (-kU + \ell V) = \rho\omega^2$$

Subtracting the second from the first of these equations, it is seen that

$$\left( \frac{Bk}{U} + \frac{B\ell}{V} \right) (-kU + \ell V) = 0 \quad (7.26)$$

Either or both of these factors equal to zero will satisfy 7.26, so that two values of  $\frac{V}{U}$  are obtained. By substituting back into equations (7.25), conditions on  $\omega^2$  are found. The two solutions will be

$$\frac{V_1}{U_1} = -\frac{\ell_1}{k} \text{ with } (A + B)(k^2 + \ell_1^2) = \rho\omega^2 \quad (7.27)$$

$$\frac{V_2}{U_2} = \frac{k}{\ell_2} \text{ with } A(k^2 + \ell_2^2) = \rho\omega^2$$

By superimposing the two solutions the  $u$  and  $v$  displacements now become

$$\begin{aligned} u &= [U_1 \cos \ell_1 y + U_2 \cos \ell_2 y] \cos kx \\ v &= \left[ -\frac{\ell_1}{k} U_1 \sin \ell_1 y + \frac{k}{\ell_2} U_2 \sin \ell_2 y \right] \sin kx \end{aligned} \quad (7.28)$$

Using the relationships of Section 7.8, one may now calculate all stresses.

The argument  $k$  has purposely been kept the same for both of the superimposed solutions in order that boundary conditions at  $y = \pm \frac{b}{2}$  might be satisfied regardless of  $x$ .

For  $Y_v$  to equal zero at the edges of the strip

$$\frac{\partial v}{\partial y} + \sigma \frac{\partial u}{\partial x} \Big|_{y=\pm \frac{b}{2}} = 0 \quad (7.29)$$

This gives rise to the equation:

$$U_1(\ell_1^2 + \sigma k^2) \cos \ell_1 \frac{b}{2} - U_2[k^2(1 - \sigma)] \cos \ell_2 \frac{b}{2} = 0 \quad (7.30)$$

Similarly, if  $X_y = 0$  at  $y = \pm \frac{b}{2}$

$$\frac{\partial u}{\partial y} + \frac{\partial v}{\partial x} \Big|_{y=\pm \frac{b}{2}} = 0 \quad (7.31)$$

Another relation is obtained from (7.31):

$$-2\ell_1 \ell_2 U_1 \sin \ell_1 \frac{b}{2} + U_2(k^2 - \ell_2^2) \sin \ell_2 \frac{b}{2} = 0 \quad (7.32)$$

The two equations (7.30) and (7.32) will be satisfied if the determinant of the coefficients of  $U_1$  and  $U_2$  vanishes. The following transcendental equation will then be obtained; values of  $\ell_1^2$  and  $\ell_2^2$  being those required by Eq. 7.27.

$$\frac{\cot \ell_1 \frac{b}{2}}{\cot \ell_2 \frac{b}{2}} = \frac{-2\ell_1 \ell_2 k^2(1 - \sigma)}{(\ell_2^2 - k^2)(\ell_1^2 + \sigma k^2)} \quad (7.13)$$

By using either of equations (7.30) and (7.32), one may derive the relation between  $U_2$  and  $U_1$  provided a solution to (7.13) is found.

$$U_2 = U_1 \frac{-2\ell_1 \ell_2 \sin \ell_1 \frac{b}{2}}{(\ell_2^2 - k^2) \sin \ell_2 \frac{b}{2}} \quad (7.33)$$

To solve equation (7.13) assume a value for  $k^2$  and plot graphically the right and left hand expressions as functions of  $\theta^2 = \frac{\rho\omega^2}{A}$ . Roots are indicated

by the crossover points. Values of  $\theta^2$  corresponding to different values of  $k^2$  may also be found in this way and a curve plotted for  $\theta^2$  versus  $k^2$ , (or for  $\theta \cdot b$  versus  $k \cdot b$ ).

### 7.92. Thickness Shear Vibrations

To obtain a formula for the approximate resonant frequencies of thickness shear for a plate having large ratios of  $\frac{W}{T}$  and  $\frac{L}{T}$ , one may consider the following displacements:

$$\begin{aligned} u &= U \sin kx \cos \ell y \cos rz \\ v &= 0 \\ w &= 0 \end{aligned} \tag{7.34}$$

If there are no cross couplings between shear stresses or between shear and extensional stresses one may write:<sup>8</sup>

$$\begin{aligned} X_x &= c_{11} \frac{\partial u}{\partial x} + c_{12} \frac{\partial v}{\partial y} + c_{13} \frac{\partial w}{\partial z} = c_{11} kU \cos kx \cos \ell y \cos rz \\ X_y &= c_{66} \left( \frac{\partial u}{\partial y} + \frac{\partial v}{\partial x} \right) = -c_{66} \ell U \sin kx \sin \ell y \cos rz \\ X_z &= c_{55} \left( \frac{\partial u}{\partial z} + \frac{\partial w}{\partial x} \right) = -c_{55} rU \sin kx \cos \ell y \sin rz \end{aligned} \tag{7.35}$$

Substituting into the first of the equilibrium equations (7.1) and dividing through by common factors

$$c_{11} k^2 + c_{66} \ell^2 + c_{55} r^2 = \rho \omega^2 \tag{7.36}$$

The other two of equations (7.1) may be neglected if  $k$  and  $r$  are quite small so that it will only be necessary to consider equation (7.36) which can be solved for  $\omega^2$ . It will be noticed that the  $X_y$  shear stress will predominate under these restrictions on  $k$  and  $r$ . Letting  $k = \frac{n\pi}{L}$ ,  $\ell = \frac{m\pi}{T}$ , and  $r = \frac{p\pi}{W}$  ( $n$ ,  $m$  and  $p$  are integers) in order to satisfy the boundary conditions for this stress and also for  $X_x$ , one obtains the following formula. (This choice of  $k$ ,  $\ell$ , and  $r$  is also required if the shear stress is to vary in essentially the same manner as is experimentally observed.)

$$\omega = 2\pi f = \pi \sqrt{\frac{1}{\rho} \sqrt{\frac{c_{11}n^2}{L^2} + \frac{c_{66}m^2}{T^2} + \frac{c_{55}p^2}{W^2}}} \tag{7.17}$$

in which  $L$  and  $W$  must be much larger than  $T$ .

<sup>8</sup> Refer to equation (7.18) for values of  $c$  constants for isotropic case.

The boundary condition for the extensional stresses will not be met; however, they will be quite small in comparison to  $X_v$  if  $k$  is small, and may be neglected.

### 7.93. Thickness Flexures

Consider a three dimensional plate having a thickness  $b$  lying along the  $y$  direction. The following displacements are found to be of a form that can be made to satisfy the equilibrium equations 7.2.

$$\left. \begin{aligned} u &= U \sin kx \sin \ell y \cos mz \\ v &= V \cos kx \cos \ell y \cos mz \\ w &= W \cos kx \sin \ell y \sin mz \end{aligned} \right\} \quad (7.37)$$

Performing the operations indicated and substituting into the equilibrium equations give the following result:

$$\left. \begin{aligned} A(k^2 + \ell^2 + m^2) + \frac{Bk}{U} (kU - \ell V + mW) &= \rho\omega^2 \\ A(k^2 + \ell^2 + m^2) - \frac{B\ell}{V} (kU - \ell V + mW) &= \rho\omega^2 \\ A(k^2 + \ell^2 + m^2) + \frac{Bm}{W} (kU - \ell V + mW) &= \rho\omega^2 \end{aligned} \right\} \quad (7.38)$$

Subtract the second and third equations of (7.38) from the first:

$$\begin{aligned} \text{then} \quad \frac{Bk}{U} + \frac{B\ell}{V} &= 0 \quad \text{and} \quad \frac{Bk}{U} - \frac{Bm}{W} = 0 \\ \text{or} \quad \frac{V}{U} &= -\frac{\ell}{k} \quad \text{and} \quad \frac{W}{U} = \frac{m}{k} \end{aligned} \quad (7.39)$$

Putting these values back into 7.38, it is seen that the following relationship must be satisfied.

$$(A + B)(k^2 + \ell^2 + m^2) = \rho\omega^2 \quad (7.40)$$

Letting  $\frac{V}{U} = -\frac{\ell}{k}$  as in (7.39), another value for  $\frac{W}{U}$  may be obtained.

The first and second equations of (7.38) will be satisfied for any ratio of  $\frac{W}{U}$ , so the 3rd equation is used.

$$A(k^2 + \ell^2 + m^2) + B\left(k^2 + \ell^2 + m\frac{W}{U}\right) = \rho\omega^2 \quad (7.41)$$

Solving for  $\frac{W}{U}$ , using (7.41) and first of equations (7.38)

$$\frac{W}{U} = \frac{m}{k} \quad \text{and} \quad \frac{W}{U} = \frac{-k^2 - \ell^2}{mk} \quad (7.42)$$

The first ratio is the same as (7.39). For the second solution to the equilibrium equations, then the following relationships exist.

$$\frac{V}{U} = \frac{-\ell}{k} \quad \text{and} \quad \frac{W}{U} = \frac{-k - \ell^2}{mk} \quad (7.43)$$

When the above are substituted back into (7.38), it is found that<sup>9</sup>

$$A(k^2 + \ell^2 + m^2) = \rho\omega^2 \quad (7.44)$$

In a similar way, using  $\frac{W}{U} = \frac{m}{k}$  the following are obtained:

$$\frac{W}{U} = \frac{m}{k}; \quad \frac{V}{U} = \frac{k^2 + m^2}{k\ell} \quad (7.45)$$

with  $A(k^2 + \ell^2 + m^2) = \rho\omega^2$  as before. This is the second solution for  $\epsilon = 0$ .

The three different solutions may now be combined or superimposed to give

$$\begin{aligned} u &= [U_1 \sin \ell_1 y + U_2 \sin \ell_2 y + U_3 \sin \ell_3 y] \sin kx \cos mz \\ v &= \left[ -U_1 \frac{\ell_1}{k} \cos \ell_1 y - U_2 \frac{\ell_2}{k} \cos \ell_2 y \right. \\ &\quad \left. + \frac{U_3(k^2 + m^2)}{\ell_3 k} \cos \ell_3 y \right] \cos kx \cos mz \quad (7.46) \\ w &= \left[ U_1 \frac{m}{k} \sin \ell_1 y - U_2 \frac{(k^2 + \ell_2^2)}{mk} \sin \ell_2 y \right. \\ &\quad \left. + U_3 \frac{m}{k} \sin \ell_3 y \right] \cos kx \sin mz \end{aligned}$$

In the above equations  $\ell_2^2 = \ell_3^2$  because of the double requirement of 7.44.<sup>10</sup>

It is now possible to calculate the stresses existing at any point. It is desired to choose  $U_1$ ,  $U_2$ , and  $U_3$  in such a manner that the boundary conditions at the two major surfaces of the plate are satisfied. By using the relations given in Section 7.8, the extensional stress  $Y_y$ , and the two shear stresses  $X_y$  and  $Y_z$  are calculated with the use of 7.46. They are then

<sup>9</sup> It should also be noticed that  $\epsilon = 0$  for this solution.

<sup>10</sup>  $k_1 = k_2 = k_3 = k$   
 $m_1 = m_2 = m_3 = m$

set to zero at the faces of the plate; i.e. at  $y = \pm \frac{b}{2}$ . Three equations, after simplifying, result.

For  $Y_v = 0$  at  $y = \pm \frac{b}{2}$

$$U_1 \left[ \sigma B(k^2 + \ell_1^2 + m^2) \sin \ell_1 \frac{b}{2} + A \ell_1^2 \sin \ell_1 \frac{b}{2} \right] \\ + U_2 \left[ A \ell_2^2 \sin \ell_2 \frac{b}{2} \right] - U_3 \left[ A(k^2 + m^2) \sin \ell_3 \frac{b}{2} \right] = 0 \quad (7.47)$$

For  $X_v = 0$  at  $y = \pm \frac{b}{2}$

$$U_1 \left[ 2\ell_1 \cos \ell_1 \frac{b}{2} \right] + U_2 \left[ 2\ell_2 \cos \ell_2 \frac{b}{2} \right] \\ + U_3 \left[ \ell_3 - \frac{(k^2 + m^2)}{\ell_3} \right] \left[ \cos \ell_3 \frac{b}{2} \right] = 0 \quad (7.48)$$

For  $Y_s = 0$  at  $y = \pm \frac{b}{2}$

$$U_1 \left[ 2\ell_1 m \cos \ell_1 \frac{b}{2} \right] + U_2 \left[ \left( \ell_2 m - \frac{\ell_2}{m} (\ell_2^2 + k^2) \right) \cos \ell_2 \frac{b}{2} \right] \\ + U_3 \left[ \left( \ell_3 m - \frac{m}{\ell_3} (k^2 + m^2) \right) \cos \ell_3 \frac{b}{2} \right] = 0 \quad (7.49)$$

In order for these three equations to be satisfied simultaneously a necessary condition is that the third order determinant formed by the coefficients of the  $U$ 's vanish. That is,

$$\begin{vmatrix} \left[ (\sigma B(k^2 + \ell_1^2 + m^2) + A \ell_1^2) \sin \ell_1 \frac{b}{2} \right] & \left[ A \ell_2^2 \sin \ell_2 \frac{b}{2} \right] & - \left[ A(k^2 + m^2) \sin \ell_3 \frac{b}{2} \right] \\ \left[ 2\ell_1 \cos \ell_1 \frac{b}{2} \right] & \left[ 2\ell_2 \cos \ell_2 \frac{b}{2} \right] & \left[ \left( \ell_3 - \frac{(k^2 + m^2)}{\ell_3} \right) \cos \ell_3 \frac{b}{2} \right] \\ \left[ 2\ell_1 m \cos \ell_1 \frac{b}{2} \right] & \left[ \left( \ell_2 m - \frac{\ell_2}{m} (\ell_2^2 + k^2) \right) \cos \ell_2 \frac{b}{2} \right] & \left[ \left( \ell_3 m - \frac{m}{\ell_3} (k^2 + m^2) \right) \cos \ell_3 \frac{b}{2} \right] \end{vmatrix} = 0 \quad (7.50)$$

By dividing row 1 by  $\cos \ell_1 \frac{b}{2}$ , row 2 by  $\cos \ell_2 \frac{b}{2}$ ; row 3 by  $\cos \ell_3 \frac{b}{2}$  and by subtracting the elements of row 3 from those of row 2, considerable simplification results.

The full expansion gives the following equation, after further simplifying operations are performed.

$$\left[ (\sigma B(k^2 + \ell_1^2 + m^2) + A\ell_1^2) \tan \ell_1 \frac{b}{2} \right] \cdot [\ell_3^2 - k^2 - m^2] + 2\ell_1 \ell_3 \left[ A(k^2 + m^2) \tan \ell_3 \frac{b}{2} \right] = 0 \quad (7.51)$$

It should be noticed that  $\ell_2$  has dropped out entirely. Actually  $\ell_2 = \ell_3$  as previously explained. Also the expression

$$\left[ \ell_2 m + \frac{\ell_2}{m} (\ell_2^2 + k^2) \right]$$

must not be zero, for in simplifying equation (7.51) it was used as a divisor.

Equation (7.51) may be rewritten to give

$$\frac{\tan \ell_1 \frac{b}{2}}{\tan \ell_3 \frac{b}{2}} = \frac{-2\ell_1 \ell_3 A(k^2 + m^2)}{[\sigma B(k^2 + \ell_1^2 + m^2) + A\ell_1^2][\ell_3^2 - k^2 - m^2]} \quad (7.52)$$

In the above

$$\left. \begin{aligned} (A + B)(k^2 + \ell_1^2 + m^2) &= \rho\omega^2 \\ A(k^2 + \ell_3^2 + m^2) &= \rho\omega^2 \end{aligned} \right\} \quad (7.53)$$

By letting  $\theta^2 = \frac{\rho\omega^2}{A}$  and  $k^2 + m^2 = \alpha^2$  equations (7.52) and (7.53) above become

$$\frac{\tan \ell_1 \frac{b}{2}}{\tan \ell_3 \frac{b}{2}} = \frac{-2\ell_1 \ell_3 A\alpha^2}{[\sigma B(\ell_1^2 + \alpha^2) + A\ell_1^2] \cdot [\ell_3^2 - \alpha^2]} \quad (7.22)$$

with

$$\begin{aligned} \ell_1^2 &= \theta^2 \cdot \frac{A}{A + B} - \alpha^2 \\ \ell_2^2 &= \ell_3^2 = \theta^2 - \alpha^2 \end{aligned}$$

Equation (7.22) represents the general solution for normal thickness vibrations in an isotropic plate of finite thickness extending to infinity in both major directions. The analogy for plates of finite dimensions is considered in the text.

## CHAPTER VIII

# Principles of Mounting Quartz Plates

By R. A. SYKES

### INTRODUCTION

**I**T IS the object of this chapter to show some of the fundamental considerations involved that govern the design of mountings or holders of quartz crystals. This discussion is restricted to the three common types, namely, rod or clamp type, wire type and airgap type. The development of these three types of mountings for applications in telephone transmission and radio systems has led to many and varied forms. Commercial designs of units for telephone uses employing these principles are described in detail in a later chapter.

In chapter VI regarding the vibrations of crystals we have assumed in all cases that the crystal is free to vibrate. In order that this condition shall be fulfilled it is necessary that any mounting which supports the crystal shall not restrict its vibration or at most the effect shall be made as negligible as possible.

### 8.1 CLAMP TYPE SUPPORTS

Of the known types of vibration it is noticed in all cases that there have been nodal points. These points by definition are points of zero motion and in all cases that we have studied appear to be single isolated points or lines of very small size in comparison with the total crystal area. The obvious type of mounting is then one which simply clamps the crystal with a very small area at these points or nodes. The early type of mountings for low-frequency crystals were all based on this principle and the area of the clamp was determined experimentally by reducing it until, with sufficient pressure to hold the crystal, a good  $Q$  was obtained. The first mountings consisted simply of two pressure points located as nearly as possible to the nodal point. It was apparent at first that this type of mounting allowed the crystal to rotate about the mounting axis and very shortly the plating or electrode open-circuited. With the development of the “-18 degree X-cut” crystal it was found that the nodal region of a longitudinally vibrating crystal was a nodal line and permitted the use of a knife-edged type of mounting instead of the single point. This type of pressure mounting was used with this crystal for quite a number of years in the crystal filters for carrier systems and is shown in Fig. 8.1. This consists mainly of four pressure edges whose

dimensions along the length of the crystal are small and width sufficiently large to insure a rigid clamp. Pressure was applied by a phosphor bronze spring in the center of the two top pressure points. This gave a satisfactory mounting and also allowed the use of a divided plating necessary for the balanced type crystal filters. This type of mounting was used in crystals of relatively low frequency, for example, 60 to 150 kc. of the "—18 degree X-cut" type.

With the use of higher-frequency crystals of different types of vibration than that described above, it has been found that this method of mounting has not been very satisfactory. In order to reduce the size of the mounting in proportion to the decreased crystal area it would be a delicate mechanical job and quite costly. This type of mounting could not be used for crystals which did not employ this type of vibration, for example the face shear type

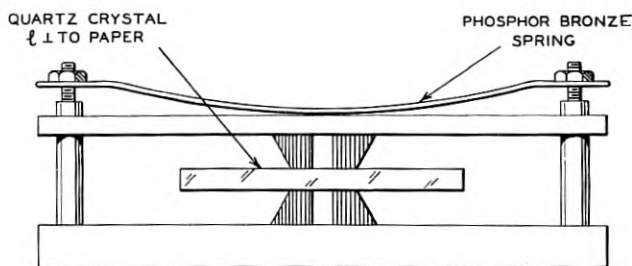


Fig. 8.1—Pressure mounting for extensional crystals.

such as the *CT* and *DT*, since there is only one spot near the center which would permit clamping at all.

To permit a crystal to vibrate freely the object used to support the crystal and maintain contact to the plated surfaces must have a very low mechanical impedance. At the same time it should possess sufficient rigidity that the complete assembly may be shocked without changing characteristics of the crystal as an oscillator. For example, if a rod or bar is held against a crystal at any point we would expect that the crystal in an oscillating condition would tend to generate motion in the bar and as this bar is placed closer to the nodal point we would expect the motion to be less. It can be seen that there are two objects to be accomplished in mounting a crystal: First, that the support must be placed as close as possible to a nodal point; and second, that the support shall have a very low mechanical impedance. This mechanical impedance needs to be low only at or near the operating frequency of the crystal. One type of support which would meet this requirement is that of a rod in flexure a discussion of which is given in Chapter VI. In this case, however, we may clamp one end of the bar and allow the other end to

be free to vibrate. This free end would then be in contact with the surface of the crystal. If the bar were clamped and were of a length such that its frequency of resonance equalled that of the crystal or approximately so, it would require very little energy from the crystal to drive it, and any energy received from the crystal would be reflected from the clamped end of the bar and thereby kept within the vibrating system. This type of support is shown in Fig. 8.2, where  $l$  = length of the rod and  $d$  its diameter. The slightly rounded end is to allow the rod to seat firmly on the crystal surface. An enlarged view of Fig. 8.2 is shown in Fig. 8.3 and shows how the rod would vibrate. Figure 8.3A shows the type of motion for the first mode of a clamp-

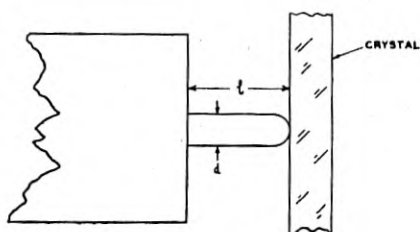


Fig. 8.2—Cantilever type mounting.

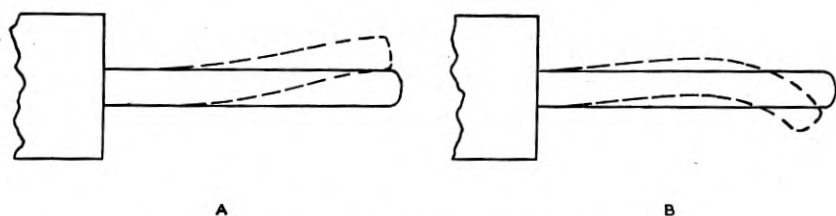


Fig. 8.3—Type of motion in cantilever support mountings.

free bar. Figure 8.3B shows the type of motion of the same bar vibrating in its second mode. This would indicate that for a given length of bar we could use it at several different frequencies by simply using higher orders of vibration. By using a clamp type mounting where the clamping rods are designed as shown in Fig. 8.2, we may now have a mounting which at the crystal frequency will allow the crystal to vibrate unrestricted but at the same time provide a very secure clamp thus preventing the crystal from moving about in its holder. To prevent rotation of the crystal about the axis of the clamped points, more than two can be used provided they are of the proper design. The frequency of a clamp-free rod in flexure is given by equation (8.1) where  $m$  now has values different than in the case of free-free flexure.

$$f = \frac{m^2 v}{8\pi l^2} \quad (8.1)$$

where  $v$  = velocity in cm./sec.

$d$  = diameter in cm.

$l$  = length in cm.

$m = 1.875$  for first mode

$= (n-1/2)\pi$  for 2nd, 3rd, etc.

From this we can compute the length necessary for a given rod at a given frequency and use this for the design of the clamping rods. This length is given in equation (8.2) for the case of a 100-kc crystal using phosphor bronze rods 1 millimeter in diameter

$$l = 1.875 \sqrt{\frac{.1 \times 36 \times 10^5}{8\pi \times 10^5}} \quad (8.2)$$

$$= .225 \text{ cm}$$

This corresponds to the case of Fig. 8.3A. For the case of Fig. 8.3B, the length is given by

$$l = .567 \text{ cm}$$

Using this same diameter rod, if we should go to a considerably higher frequency, for example 5 megacycles, the value of  $l$  would be extremely small even for the case of Fig. 8.3A and would be somewhat smaller than the diameter of the rod. As mentioned before in Chapter VI, the simple formulae that apply in the case of flexure are only for the case of a long thin rod. When the length becomes equal to or less than this diameter, it is very probable that the support member should be designed as though it were vibrating in shear. These follow well-known rules and are only mentioned here in case designs for high-frequency crystals are contemplated using this method.

The design of rod-supported crystals following this procedure has not been carried on to a large extent in these laboratories because, at present, the wire-supported crystal appears to have many advantages. A great deal more of the work in regard to resonating supports has been done for the case of the soldered lead type<sup>1</sup>.

## 8.2 WIRE TYPE SUPPORTS

The theory of resonating supports involving soldered leads on crystals is very similar to that just discussed for the case of rods. There are two additional elements that we have here that are not present in the case of the rod, these elements being the actual solder connections that fasten the wire

<sup>1</sup> The presence of standing waves on the lead wires of CT crystals was found experimentally by Mr. I. E. Fair.

to the crystal and the coupling between the crystal and wire vibrating systems. Considerable work has been done in regard to the amount of solder necessary and the most desirable shape for the solder cone. The complete assembly of a wire support for a crystal is shown in Fig. 8.4. The shape of the solder cone shown in Fig. 8.4 has proved to be the most desirable and has been termed as "bell-shaped." This type of cone formation allows the wire to be twisted in handling and still not break away the top of the cone and form an appreciable crater. For the purposes of analysis we may then assume that the cone becomes part of the crystal and moves with it so that when computing the length of a wire vibrating in flexure, this length should be determined from the top of the cone. The amount of solder used in the cone since it is part of the crystal must be kept at a minimum in order that the constants of the crystal equivalent circuit will not be modified too much by it. One established fact of the effect of the solder in the cone on the

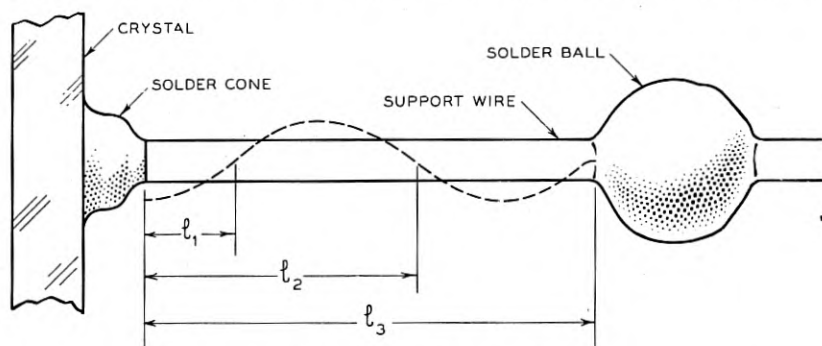


Fig. 8.4—Soldered lead type mounting.

equivalent circuit is to raise the resistance in the equivalent circuit for the crystal and this resistance increases considerably with an increase in temperature. The amount of solder permissible in the cone would then be determined by the maximum temperature at which the crystal is to be operated and the minimum  $Q$  allowable. The type of motion that the crystal would generate in the support wire when oscillating is that shown in Fig. 8.4 by the dotted line. The solder ball shown to the right of the figure acts as the clamp for the wire. This solder ball may be placed at any point along the wire corresponding to a node. The diameter of this ball need only be sufficient to act as a clamp. In general, this will be in proportion to the wire diameter. For example, at 200 kc it was necessary to use a solder ball 60 mils in diameter on a 6.0-mil diameter phosphor bronze wire. The spacing between the solder ball and the head of the cone may be readily computed from equation (8.1). In practice, it has been found that in most all cases this distance is slightly greater than that given by the formula due to the

fact that the free end is restricted to zero slope and for a given crystal and support wire it should be determined experimentally using the values obtained from equation (8.1) as a guide in the design. The diameter of the solder ball that acts as a clamp may also be determined experimentally by

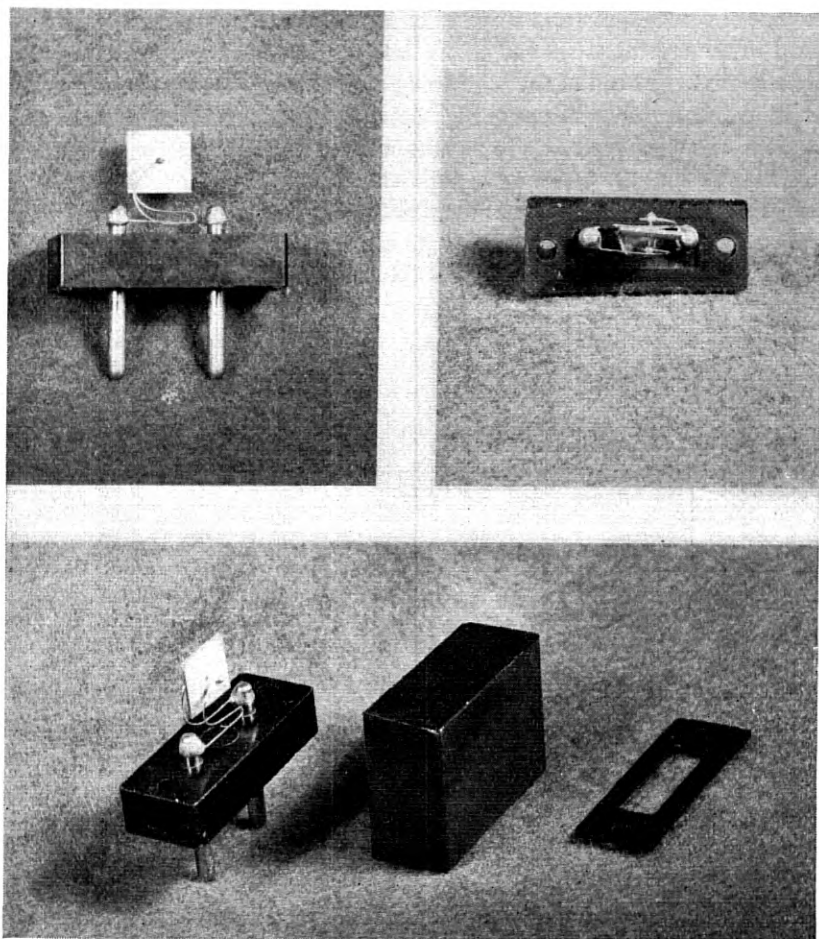


Fig. 8.5—FT-241 crystal mounting.

increasing its size until the standing waves on the wire to the right of the ball are sufficiently reduced. A practical application of this type of support is shown in Fig. 8.5. The top view shows the small wires soldered to the crystal as well as the solder balls that are spaced at points corresponding to the second node on the lead wire from the crystal. These solder balls act

as mechanical termination for the lead wires and also as connection to larger size spring wires forming the rest of the shock-proof mounting.

Another type of wire support that has found considerable practical use and is superior to the straight lead and solder cone type of connection is that of the headed wire. This is shown in Fig. 8.6. A headed wire is similar to that of common pin and may be connected to the crystal by sweating the head to the crystal as shown. This has certain advantages over the solder cone in that the head of the wire being a machined part is always constant and the distance  $d$ , as shown in Fig. 8.6, is the same for all mountings. The amount of solder necessary to sweat the head to the crystal is considerably less than in the case of the cone and hence this type of mounting will have less dissipation at the higher temperatures. One other factor not mentioned above is that the coupling between the vibrating system of the wire and the vibrating system of the crystal is considerably reduced by the use of

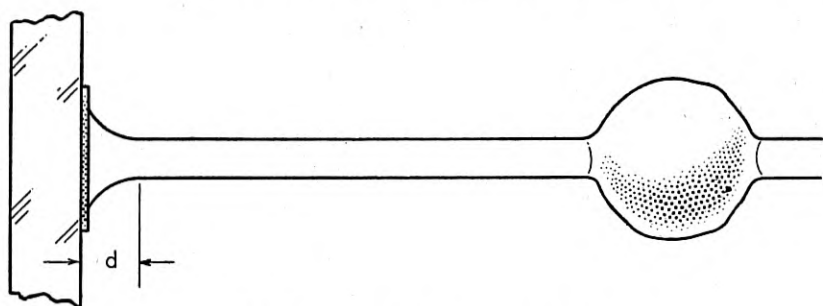


Fig. 8.6—Headed wire type mounting.

the headed wire. This is an important factor in reducing what may be termed a double system of standing waves on the wire. One standing wave system would result from reflections from the clamped end of the wire, while the other would result from reflections between the clamped wires coupled through the crystal. This may be reduced by a reduction of coupling between the crystal and wire vibrating systems.

Measurements have been made on the effect of clamping the wire-supported crystal at various points, on the activity and frequency of several different crystals used in oscillators and filters. Figure 8.7 shows the effect of clamping a 500-kc CT type crystal such as now used in the FT-241 holder. Figure 8.8 shows the same condition for a 370-kc CT crystal. It will be noted that in these two cases with the decrease in frequency of the crystal that the coupling between the wire and crystal has decreased, as shown by a smaller change in frequency and also, that for the lower frequency crystal the change in activity is modified only when the clamp is very close to a loop of motion on the wire. The mountings of these crystals were of the type

shown in Fig. 8.4 where the amount of solder in the cone equals that of a solder pellet 20 mils in diameter and 12 mils high.

Figure 8.9 shows the change in frequency as a result of clamping one wire of a four-wire mounting of a GT-cut crystal designed for use as a filter ele-

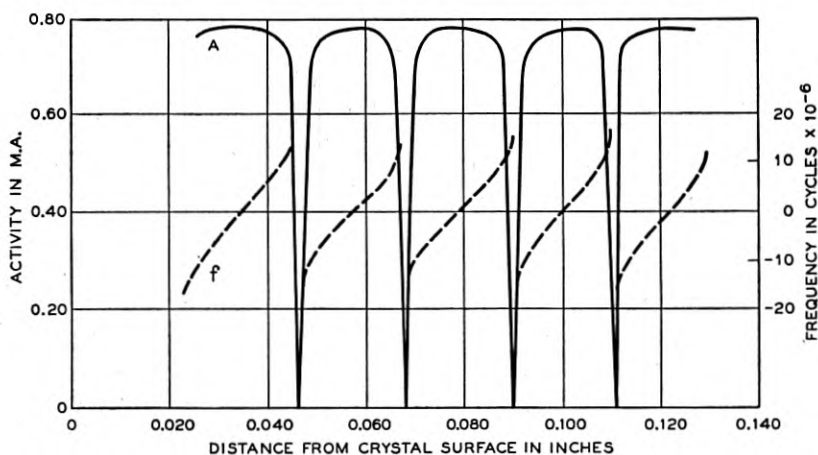


Fig. 8.7—Effect on frequency and activity of clamping one lead of 500 kc. CT-cut crystal.

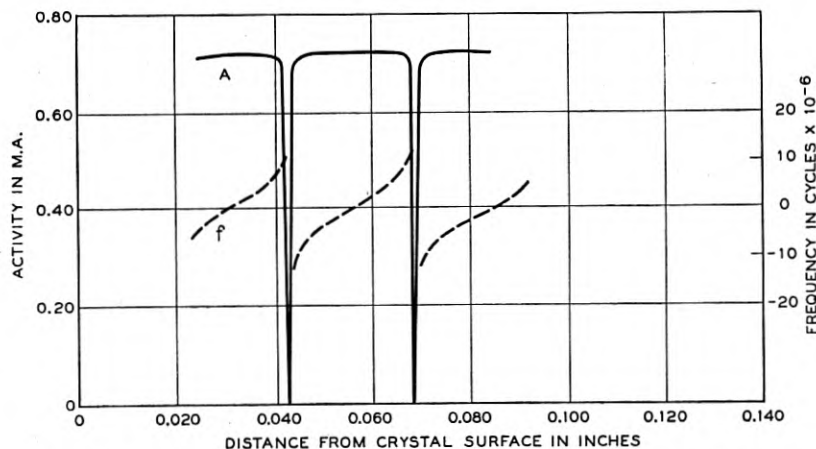


Fig. 8.8—Effect on frequency and activity of clamping one lead of 370 kc. CT-cut crystal.

ment at 164 kilocycles. This change is shown for the lower resonance at 143 kilocycles since this mode would be more affected by clamping. The large deviations in frequency correspond to clamping at the loops of the wire as shown in Figs. 8.8 and 8.9 but the small sudden changes in frequency are a result of a second system of standing waves as previously described. This

second system of standing waves results from too much coupling between the crystal and the two oppositely disposed lead wires. It may be reduced by first placing the wires closer to the nodal point and second, using a smaller amount of solder in the cone to attach the lead wire to the crystal. Measurements on this same type of crystal when the above conditions were fulfilled showed practically no effects of secondary standing waves. It is important to keep the energy transmitted to the lead wires low since a soldered connection near a loop of motion resulting from secondary standing waves on the wire will act as a clamp and will materially decrease the resulting  $Q$  of the crystal. This is probably the best reason for the use of the headed wire type of lead wherever practical.

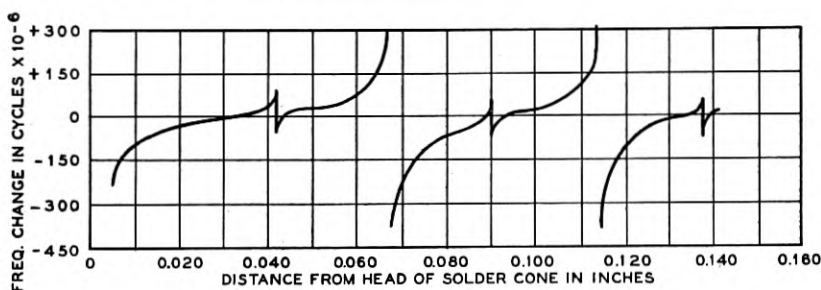


Fig. 8.9—Effect on the frequency of lower resonances of clamping one lead of 164 kc. GT-cut crystal.

### 8.3 AIR-GAP TYPE SUPPORTS

A third form of mounting for quartz crystals is that of the airgap type shown in Fig. 8.10 where the crystal plate is held between two flat electrodes. Two forms of the airgap type of mounting are shown. In Fig. 8.10A the crystal is free to vibrate between two flat electrodes held together to produce a definite airgap of thickness  $t$ . In Fig. 8.10B small lands are left on the corners of the electrodes to produce a uniform airgap on each side of the crystal as well as to clamp the crystal plate.

This type of mounting has found its greatest use for oscillator crystals of the AT and BT type. The factor that determines the choice of mount is the ratio of length to thickness of the crystal. For example, when the length is less than 20 times the thickness, clamping the corners of AT and BT type crystals will decrease the activity in proportion to the clamping pressure. This is apparent from a study of the type of motion for these crystals described in Chapter VI. This then indicates that AT and BT type crystals for broadcast frequencies should employ a mounting with the crystal unrestricted as shown in Fig. 8.10A while the higher radio frequency crystals may be clamped as shown in Fig. 8.10B. The clamping pressure will be

dependent upon the area of the crystal, its frequency and the amount of activity required. One advantage of the clamped type support lies in the fact that many of the unwanted modes of motion are restricted or dampened to the extent that they will not cause serious dips in the activity character-

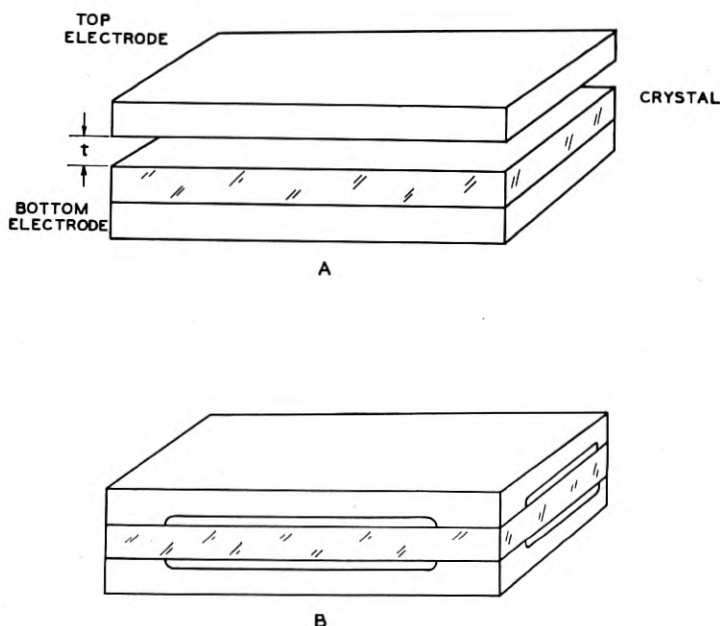


Fig. 8.10—Air gap type mounting.  
A—Crystal free.  
B—Crystal clamped at corners.

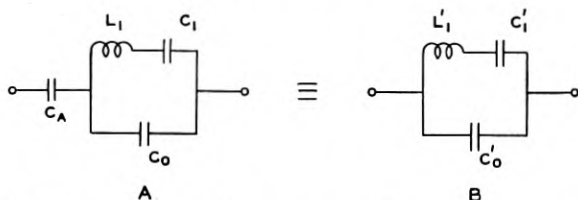


Fig. 8.11—Equivalent circuit of a quartz crystal in an air gap type mounting.

istic over a wide temperature range. This explains in part the necessity for accurate control of the length and width dimensions for crystals of low radio frequencies using the type of mounting shown in Fig. 8.10A.

The effect of the airgap on the constants of the crystal equivalent circuit may be determined from Fig. 8.11. In Fig. 8.11A is shown the usual crystal equivalent circuit in series with a capacity  $C_A$  which represents the capacity

of the airgap. This may be reduced to the circuit of Fig. 8.11B where the constants are given by

$$C'_0 = \frac{C_A}{C_A + C_0} C_0$$

$$C'_1 = \frac{C_A^2}{(C_A + C_0)(C_1 + C_A + C_0)} C_1$$

$$L'_1 = \left[ \frac{C_A + C_0}{C_A} \right]^2 L_1$$

The circuit of Fig. 8.11B is the same form as that of the original crystal and therefore we may assume that the effect of the airgap is to produce a similar

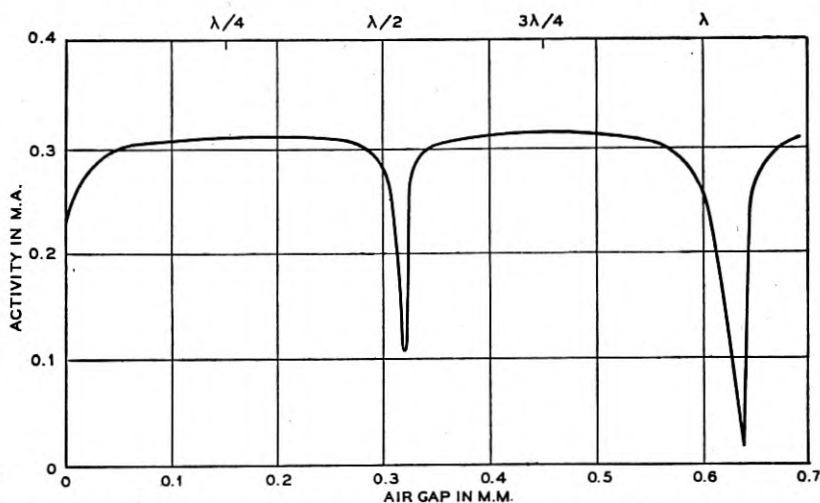


Fig. 8.12—Effect on frequency of the air gap thickness on a 550 kc. AT-cut crystal.

crystal of reduced capacity and reduced effective piezoelectric coupling. In the case of oscillatory crystals the effect of the airgap is to reduce the activity and decrease the range of frequency adjustment with parallel capacity. For filter applications the effect of the airgap is to produce narrower transmission bands and higher characteristic impedance. One other effect of the airgap results from the propagation of acoustic waves from the crystal.

It is known that most any type of crystal in a vibrating condition will produce acoustic waves in air and if an object capable of reflecting these waves is the proper distance away, these acoustic waves may be reflected back to the crystal surface. The reflections from distances corresponding to even quarter wave-lengths will cause considerable damping while the reflections from distances corresponding to odd quarter wave-lengths will

cause very little. The wave-length of a sound wave in air may be readily computed, and since we are interested in multiples of one-quarter wave-length, it is desirable to determine these for a given frequency. This can be computed readily from equation 8.3,

$$\frac{\lambda}{4} = \frac{v}{4f} \quad 8.3$$

where  $v$  is the velocity of sound in air at room temperature and pressure and equals 33,000 centimeters per second. For example, a quarter of a wave-length at 5 megacycles is given by

$$\frac{\lambda}{4} = \frac{33,000}{4 \times 5 \times 10^6} = .00165 \text{ cm}$$

which indicates that if  $t$  of Fig. 8.10 were made equal to this or odd multiples, there would be very little effect of the electrode on the crystal and if  $t$  corresponded to even multiples of a quarter wave-length, we would expect considerable damping. Some measurements of this effect have been made with a low frequency *AT*-cut quartz crystal and are shown in Fig. 8.12. The sound wave generated by an *AT*-cut probably results from flexure waves generated by the high-frequency shear wave. It will be noted that when the airgap is equal to even multiples of a quarter wave-length, the activity is considerably reduced. Further, it will be noticed that airgaps in the order of 1/8 of the wave-length may be used and produce very little effect. Since a large airgap reduces the piezoelectric coupling it is desirable to keep this about 1/8 of a wave-length as a maximum unless, in special cases, a reduction in piezoelectric coupling may be tolerated.

## The Magnetically Focused Radial Beam Vacuum Tube

By A. M. SKELLETT

A new type of vacuum tube is described in which a flat radial beam of electrons in a cylindrical structure may be made to rotate about the axis. Features of the tube are its absence of an internal focusing structure and resultant simplicity of design, its small size, its low voltages, and its high beam currents. The focusing of the beams and their directional control are accomplished by the magnetic fields in small polyphase motor stators. A time division multiplex signaling system for 30 channels using these tubes is briefly described.

**I**T HAS long been recognized that the substitution of electron beams for mechanical moving parts would offer decided advantages in many applications in the field of communications. The high voltages required for the usual cathode-ray type of tube and the very low currents obtainable therefrom prevent their use in most such proposals; their complicated guns and their large sizes are also undesirable features. The kind of tube described herein has no focusing structure, is small in size, requires only low voltages, utilizes the cathode power efficiently, and produces beam currents of the same order of magnitude as the space currents of ordinary vacuum tubes.

Figure 1 shows the elementary tube structure. It consists, in the simplest case, of a cylindrical cathode of the sort in common use in vacuum tubes, surrounded by a cylindrical anode structure. When this structure is made positive with respect to the cathode and there is no magnetic field in the tube, the electrons flow to the anode structure in all directions around the axis. When a uniform magnetic field is applied with its direction at right angles to the axis, the electrons are focused into two diametrically opposite beams as shown. The beams are parallel to the lines of force of the magnetic field so that if the field is rotated the beams move around with it. Thus the magnetic field serves both to focus the electrons and to direct the resulting beams to different elements of the anode structure.

If ordinary commercial cathodes are used with anode structures an inch or two in diameter, 100 volts or less on the anode will draw the full space current for which the cathode was designed. The application of the magnetic field will then focus from 85 to 90 per cent of this electron current into the two beams, the remaining 10 or 15 per cent being lost at the cathode due to an increase in the space charge which the magnetic field produces. Some of the smaller tubes produce beam currents of more than 5 milliamperes with only 50 volts on the anode structure, and in some of the tubes with larger cathodes beam currents of 50 milliamperes or more are easily obtainable. The magnetic field strengths range from 50 to 300 gauss.

For some applications it is desirable to eliminate one of the two beams and this may be accomplished by substituting a uniform electrical field in the tube for the cylindrical one described above. The uniform field may be obtained by applying to the anode elements a series of potentials that vary according to the sine of the angle taken around the axis. The line joining the maximum potentials (+ and -) is maintained parallel to the magnetic field so that on one side of the cathode the potentials are all negative and the

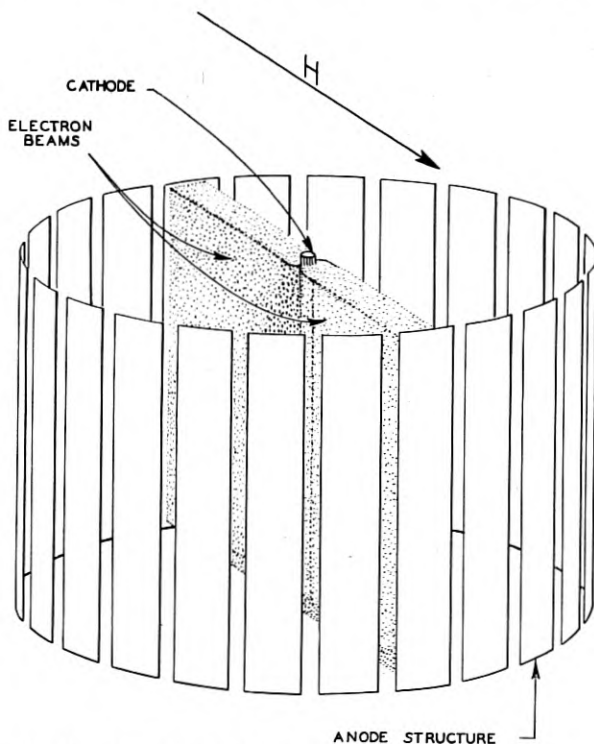


Fig. 1.—Elementary tube structure showing focused beams.

beam on that side is suppressed. The remaining beam will have somewhat less current than the corresponding one in the cylindrical field but the magnetic field-strength required for focus is reduced.

#### CYLINDRICAL ELECTRICAL FIELD

For the case of the cylindrical electric field the focus is obtained by applying a magnetic field that is strong enough to reduce the radius of curvature of the spiral electron trajectories to a small value. There is not obtained an electron optical image of the cathode in the usual sense that for

each point on the cathode there is a corresponding point on the image. The sharpness of the image may be increased by increasing the strength of the magnetic field and the field required for any degree of focus is not sharply critical.

Figure 2 shows a series of drawings of the various electron images that were obtained as the magnetic field-strength was increased in a tube having

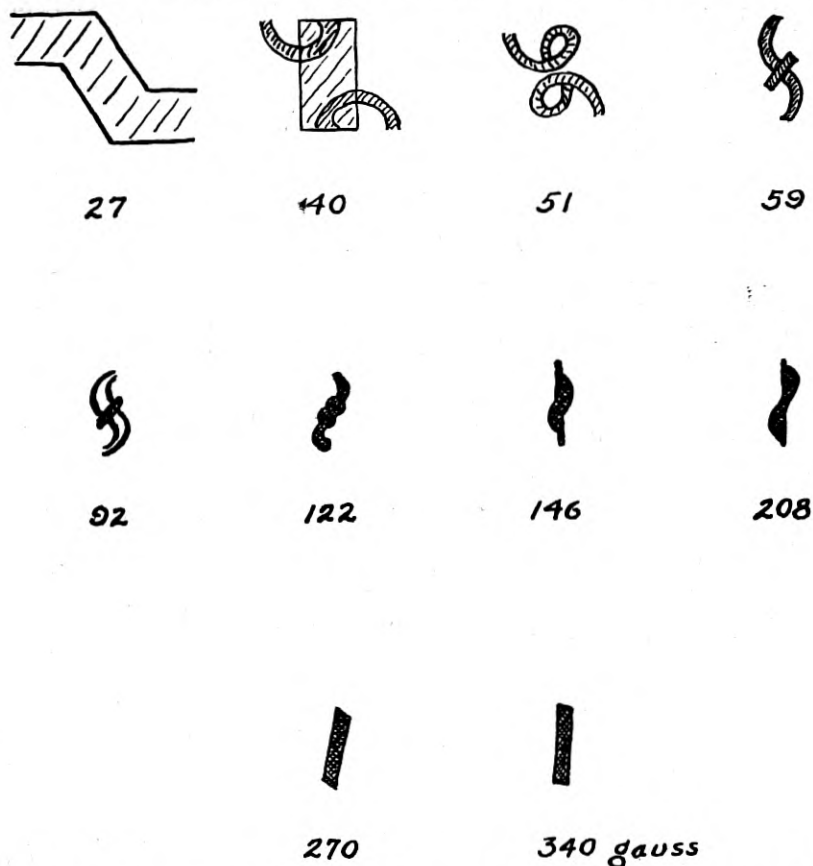
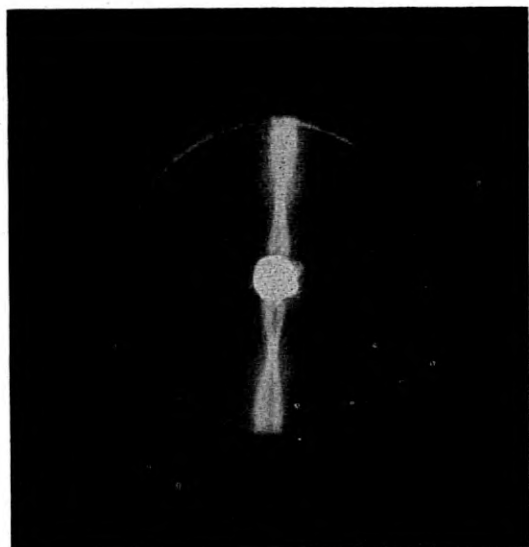
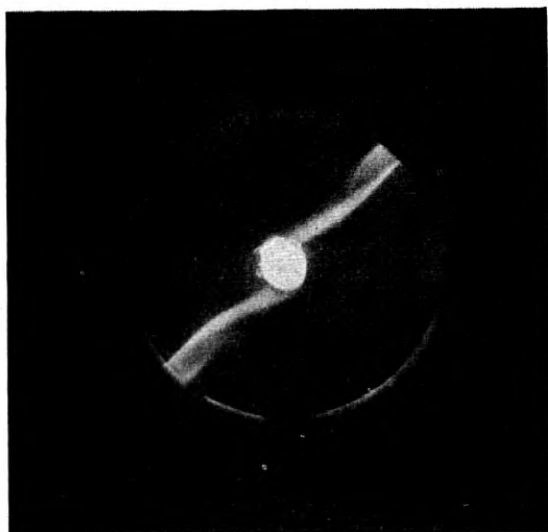


Fig. 2.—Drawings of the patterns obtained with a fluorescent coating on the inside of the anode when the magnetic field strength is increased from zero to the focus values.

a fluorescent coating on the inside cylinder. The cathode and anode diameters were 0.0625 and 2.5 inches, respectively, and the axial length was 2 inches. The anode was held at 150 volts. Only one-half inch of the cathode length, located centrally along the axis, was coated to emit electrons. The image at 340 gauss appeared to be one-half inch long. In attempting to interpret these patterns it should be remembered that on the two sides of the cathode at right angles to the plane of the beam the electrons follow



A



B

Fig. 3.—Electron trajectories made visible with a small amount of gas. A.—Magnetic field lined up with active spots on the cathode. B.—Magnetic field at  $45^\circ$  with respect to the active spots.

cycloid-like paths along the cathode, moving up on one side and down on the other.

The photographs of Fig. 3 showing the trajectories were obtained by

introducing argon at a pressure of about a micron into the tube. The electrons are emitted from only two spots of active material located at the opposite ends of a diameter on the cathode sleeve. In Fig. 3a the line joining the spots is lined up with the magnetic field and in 3b this line is at an angle of about  $45^\circ$  with respect to the field. This arrangement does not reproduce exactly the space charge conditions in the tube as actually used but does serve to give a picture of the electron paths in a qualitative sort of way.

As shown by the patterns of Fig. 2 above a minimum strength of magnetic field the shape of the focus does not change greatly. An approximate equation may be derived for the beam width in terms of the magnetic field above this minimum value that is useful for predicting the performance of new designs. The electrons that leave the cathode at right angles to the beam require the strongest magnetic field to keep them in focus. Now because of the cylindrical structure the electric field is concentrated near the cathode and we will assume that after leaving the vicinity of the cathode the velocity does not change appreciably. Setting  $v$  equal to the component of this velocity at right angles to the magnetic field we have that the radius  $r$  of the spiral path is given by the relation

$$r = \frac{mv}{eH}$$

where  $H$  is the magnetic field-strength and  $m$  and  $e$  are the mass and charge of an electron.

We also write

$$v = \sqrt{\frac{2eKV}{m}}$$

where  $K$  is the fraction of the anode voltage corresponding to  $v$ .

The width of the focus  $A$  is approximately equal to the cathode diameter  $D$  plus twice the maximum radius of curvature of the spiral paths

$$A \approx D + \frac{6.7\sqrt{KV}}{H}$$

where  $A$  and  $D$  are in centimeters and  $V$  is in practical volts. By substitution in this formula we have found that the empirical constant  $K$  is about 0.7 for the tubes that have been made to date. A minimum value for  $H$  is obtained, again approximately, by setting the last term in the equation equal to  $D$ .

#### UNIFORM ELECTRIC FIELD

As mentioned above the uniform field is obtained by imposing potentials around the anode periphery varying as the sine of the angle. The cathode is

at a point of zero potential. In this case a real electron optical image of the cathode is obtained.

Neglecting the distortion of the field in the vicinity of the cathode, the force equation for the electrons is

$$m \frac{d^2 x}{dt^2} = e \frac{V}{R}$$

where  $V$  is the maximum anode potential,  $R$  is the radius of the anode structure and  $x$  is measured in the direction of the fields. Since the acceleration is uniform the transit time  $t$ , neglecting space charge effects, may be obtained from the expression

$$\frac{1}{2} \left( \frac{d^2 x}{dt^2} \right) t^2 = R$$

Combining these equations we get

$$t = \frac{R}{\sqrt{\frac{Ve}{2m}}}$$

The condition for focus is that the electrons make one revolution around the lines of force in time  $t$ . The angular velocity of the electrons is given by the well-known expression

$$\omega = \frac{He}{m}$$

Setting  $\omega t = 2\pi$  we get

$$H = \frac{2\pi}{R} \sqrt{\frac{m}{2e} V}$$

or in practical units

$$H = \frac{10.6\sqrt{V}}{R}$$

Since the effect of the magnetic field on the space charge has not been evaluated, we can only estimate the order of magnitude of the increase of transit time due to the space charge. On the assumption that this increase introduces a factor of  $3/2^*$  the above expression with space charge is

$$H = \frac{7.1\sqrt{V}}{R}$$

This formula has been found to check well experimentally.

\* The factor of  $3/2$  is the ratio of the transit times in a plane parallel diode with and without space charge. See for example Millman and Seely, "Electronics," Chapt. 7, p. 231.

These last two formulae are for the first focus. Focii will also be obtained for values of  $H$  equal to  $nH$  where  $n$  is an integer and equal to the number of electronic revolutions. Actually as the field is increased beyond that necessary for the first focus the beam does not get very badly out of focus because the radius of curvature of the spiral path is small and for still higher fields the beam remains in approximate focus for all values of  $H$ .

In applications where the beam is rotated by means of a rotating magnetic field this electrostatic field is made to turn by separating the anode structure into four or six elements (or groups thereof) and applying either two- or three-phase alternating potentials to them.

### MAGNETIC FIELD SUPPLY

The stator of a two-pole polyphase alternating-current motor furnishes an excellent magnetic field for use with these tubes. The tube is inserted in place of the armature and when the polyphase currents are applied the beams are formed and rotate at the cyclic frequency. For applications where the beams are not rotated continuously, a two-phase stator may be used in which the currents through the two windings are adjusted to be proportional to the sine and cosine of the desired direction angle of the beam. Permanent magnets of the horseshoe design have also been found to be suitable.

The power consumed by a stator depends on its size and the strength of the field it produces and on the cyclic frequency if it is used to rotate the beam. At low frequencies, e.g., 20 or 60 cycles, the power consumed is primarily that due to the copper loss. At higher frequencies the losses in the core material become important. For some of the smaller tubes operating at a low frequency, the power consumed by the stator is less than three watts. This stator has the regular motor windings which do not completely fill the slots.

Since a polyphase source of power is not always readily available, it is sometimes advantageous to split single-phase power in the stator itself to produce the rotating field. This may be done by inserting a condenser in series with each winding so that the current through one phase winding lags by  $45^\circ$  and that through the other leads by an equal angle. Polyphase potentials for producing a rotating electrostatic field in the tube may then be taken from the windings of the stator if desired.

### TUBE DESIGN

The particular design of tube depends on its application. The simple design shown in Fig. 1 has been found adequate for some purposes but more elaborate designs which increase the versatility of the tube are also needed.

Figure 4 shows a tube with 30 anodes that incorporates various auxiliary elements. This tube is 2.25 inches in diameter. Figure 5 shows the internal

arrangement of the elements. Closely surrounding the cathode is a control grid that may be used for modulating the current density of the electron beams. Farther out is a cylindrical element with 30 windows that is maintained positive and which by virtue of its similarity in position to the third element of a tetrode is called a screen. Immediately behind each window there is a pair of paraxial wires which because of its similarity in function to the fourth element of a pentode is called a suppressor grid. In back of each suppressor grid there is an anode. In this particular tube there are pro-

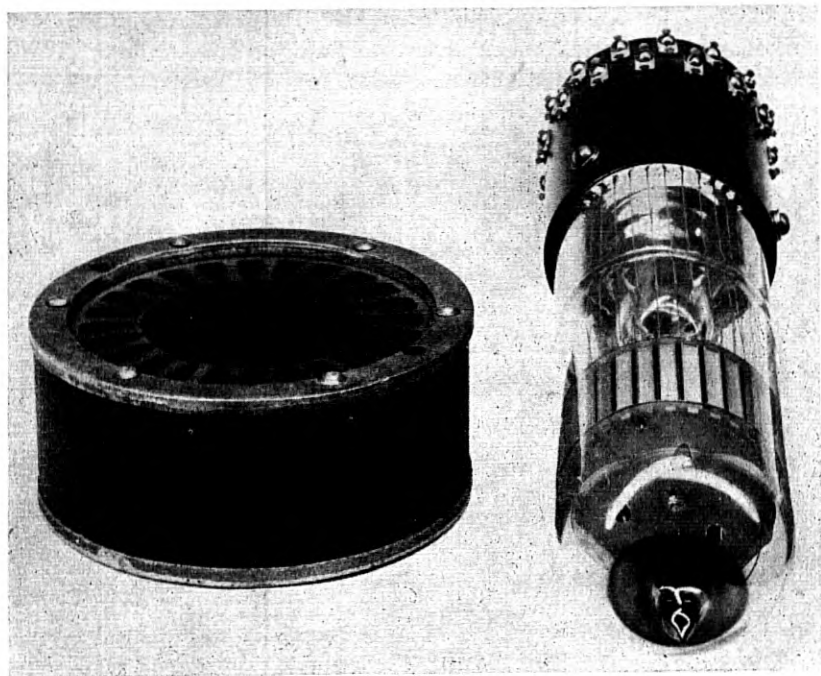


Fig. 4.—Radial beam tube with 30 anodes and unwound stator used with it.

jections like gear teeth on the back of the screen element to prevent electrons, destined for one anode, from reaching an adjacent one.

The control grid that is close to the cathode is biased negatively and controls the electron current in the same way that it would if the magnetic field were not present. The space current vs. grid potential curve is nearly identical for the two cases: with and without the magnetic field. The slight difference is due to the fact that the presence of the magnetic field increases the space charge near the cathode. Thus the tube may be used for amplification in the usual way when the electrons are focused. The presence of this grid has no appreciable effect on the focusing of the electrons.

Since the screen element is in one piece there will be present two beams out to it. One of these may be suppressed after it has passed through the screen by the suppressor grids or by the anodes in the manner described below.

These suppressor grids are generally operated at cathode potential or at a potential that is negative with respect to the cathode. They may be used for three purposes: to suppress secondaries from the anodes, to modulate the beam current to their particular anode, and to suppress one of the two beams. For the first of these functions they are biased at cathode potential. For the second they are biased negatively and have a modulation curve similar to that of the suppressor grid in a pentode. Curve A of Fig. 6 shows the variation of beam current to one anode when the potential of the suppressor grid in front of it is varied. This curve is for a grid similar to the two paraxial

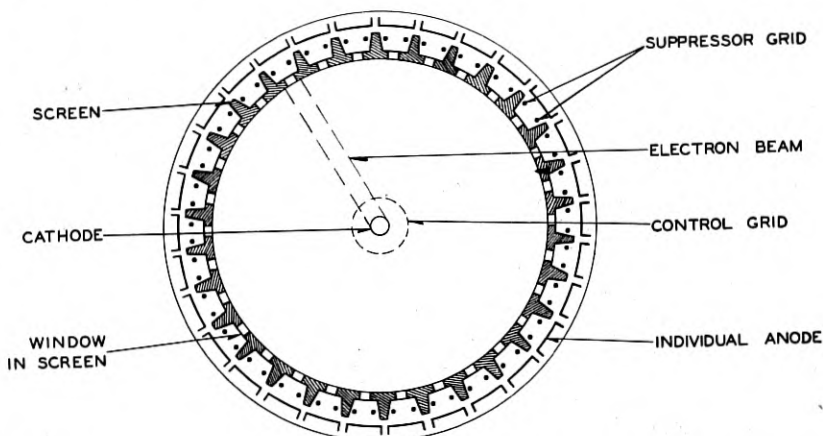


Fig. 5.—Arrangement of elements in the tube shown in Figure 4. Only the operating beam is shown.

wires in the tube shown in Fig. 5. For some applications a higher suppressor-anode transconductance or a lower cut-off is desirable and these may be obtained by welding lateral wires across this grid window to make the grid action more effective. Curve B of Fig. 6 was taken with the same size window across which laterals were welded. The table below gives the data for this suppressor grid with and without the lateral cross wires.

	Without Laterals	With Laterals
Transconductance (mho).....	100	250
Anode Resistance (ohms).....	30,000	64,000
Amplification Factor.....	3.5	16.0
Cut-Off Voltage.....	-80	-20

It is apparent from these data that amplification of the signals applied to the individual suppressors may be readily obtained.

If the screen element is split to give a uniform electrostatic field to suppress one beam, the beam current is only about half that of one beam of the cylindrical field case. This is because with the uniform electrostatic field the potential gradient at the cathode decreases with azimuthal angle away from the beam axis. If the unwanted beam is rejected by the suppressor grids, however, the beam current for the cylindrical case is obtained since the screen in this latter case supplies a cylindrical electrostatic field at the cathode and the unwanted beam is rejected between the screen and suppressor grids.

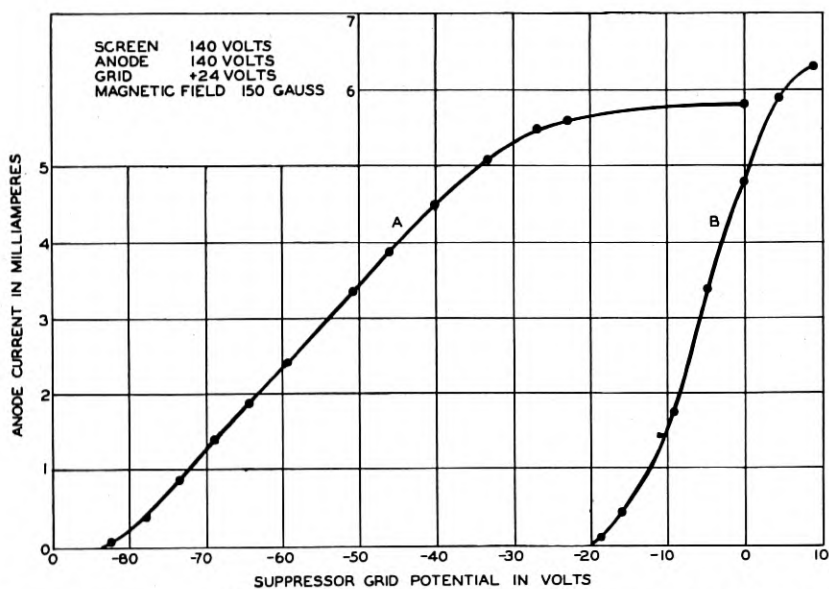


Fig. 6.—Suppressor grid characteristics. A.—Without lateral wires. B.—With lateral wires.

For this case the screen is maintained at the same positive potential required for the two-beam condition and the suppressors are so biased that they are beyond cut-off on one side of the tube and at or near cathode potential on the other side. If the beam is rotated the suppressors are connected to the polyphase supply in groups in the same way that the screen elements would be connected except that the d-c. bias above and below which the a-c. potentials swing is made negative at a value near cut-off for the suppressors.

When one beam is suppressed either by splitting the screen or by grouping the suppressors, the currents to the different anodes are not all exactly the same. For instance, maximum current will be received by an anode back

of the center of one of the screen elements or one of the suppressor groups and a minimum current will be received by an anode back of the junction of two such elements or groups. If two-phase supply is used (4 elements or groups) the ratio of maximum to minimum anode current will be 0.707 and for three-phase supply this ratio will be 0.866. There will be 4 or 6 maxima, respectively, around the tube. This variation may be effectively eliminated by varying the individual anode load impedances or in other ways.

The anode characteristics are similar to those of a pentode if suppressor grids are used and to that of a tetrode if these grids are not used.

There is still another method of effectively eliminating one beam. This consists in using an odd number of anodes so that when one beam is focused on an anode the opposite one falls on the screen in between two anode positions. With this type of tube the effective rotational frequency is twice the cyclic frequency of the rotating field, that is, all of the anodes are contacted twice (once for each beam) per revolution of the field.

#### APPLICATIONS

The many possible combinations of the tube elements just described permit a variety of applications. One of the simplest and most obvious is that of an electronic commutator which has the advantages over the corresponding mechanical device of speed and freedom from contact trouble. There is, however, a practical limitation to the speed of this electronic commutator that is set primarily by the alternating-current losses in the stator. This is estimated to be in the neighborhood of 10,000 cycles per second for ordinary stator and tube designs. The highest cyclic speed for a stator that has been used to date was 600 cycles per second which with utilization of both beams gave an effective cyclic frequency of 1200 cps.

One of the earliest systems of multiplex telegraphy was based on time division using mechanical rotating commutators. A small portion of the time of one cycle of the moving brush was allotted to each channel. The usefulness of this system is limited because of the faults of the mechanical commutators. The substitution of these electronic commutators eliminates these difficulties and puts the time division system on a more practical basis. It has an advantage over the frequency division multiplex system (carrier system) in that the elaborate filters of the latter are not required.

A 30-channel multiplex system for signaling using two of the 30 anode tubes described above has been successfully tested over short distances in the metropolitan area in New York City. The tube at the transmitter had all of the anodes tied together and the signal from them was sent over the line. The 30 input channels terminated on the suppressor grids of this tube. At the receiver, the input was fed to the negative grid surrounding the cathode and each of the anodes was connected in series with a small neon lamp for

an indicator. A signal on any one or signals on any group of the 30 input channels would actuate the corresponding lamp or lamps at the receiver. No amplification other than that provided by the receiver tube was needed.

A single beam was used in each tube, the other one being rendered ineffective in the transmitter by means of two-phase potentials applied to the

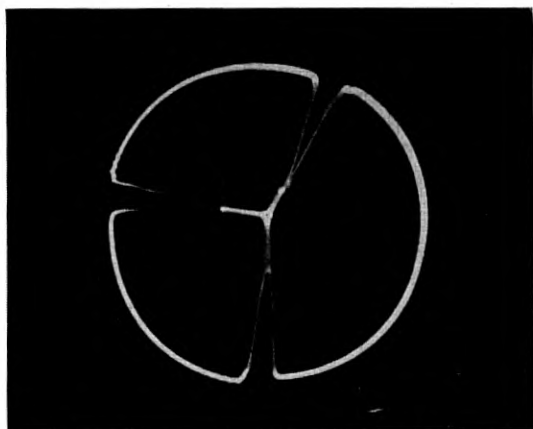


Fig. 7.—Circular trace oscillograph of transmitted signal when 3 out of 30 channels are in operation.

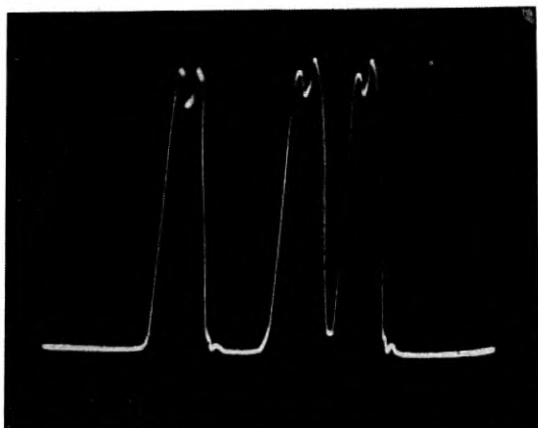


Fig. 8.—Linear trace oscillograph showing transmitted signal with 3 channels in operation 2 of which are adjacent.

suppressors in the manner described above and in the receiver by means of a combination of d-c. and two-phase a-c. potentials applied to the individual anodes. The potential of an anode was zero when the unwanted beam arrived and at or near 200 volts at the time of passage of the operating beam. The rotational frequency of the beam was sixty cycles and since both

stators were tied into the same source of power, no separate synchronizing means was necessary.

Figure 7 is a photograph of the cathode ray trace of the output of the transmitter tube when signals were being sent over three channels. A circular sweep circuit was used which distorted the signals somewhat. The shape of the pulses is shown better in Fig. 8 for which a linear sweep was employed. Signals were put on three channels, two of which were adjacent. The double-humped top of the pulse is caused by the window in the screen being slightly narrower than the beam width so that as the beam crosses the window, the greater densities in the edges relative to the center give this shape. A flat-topped pulse may be obtained by making the windows wider than the beam.

In conclusion the writer wishes to acknowledge his indebtedness to a number of his colleagues in the Laboratories for aid in the development of the tube. The 30-channel multiplex system was set up with the aid of Mr. W. H. T. Holden.

## Abstracts of Technical Articles by Bell System Authors

*A Modification of Hallén's Solution of the Antenna Problem.*<sup>1</sup> M. C. GRAY. An alternative formula for the input impedance of a cylindrical antenna is derived from Hallén's integral equation. It is shown that the introduction of a variable parameter  $Z(z)$  in place of Hallén's  $\Omega = \log(4l^2/a^2)$  modifies the numerical results considerably, and leads to much better agreement with experimental evidence.

*Motor Systems for Motion Picture Production.*<sup>2</sup> A. L. HOLCOMB. The various types of motor systems and speed controls used in motion picture production are reviewed, evaluated, and the basic theory of operation described.

Motor drive systems are a fairly simple but important element in the production of motion pictures, but to many people who do not have direct contact with this phase of activities, the number of systems in use and their peculiarities are very confusing. Data on most of the different types of motors and motor systems in use have been published, but in different places and at different times so that no comprehensive reference exists. This paper is not intended as information on new developments or as a technical study, but rather as a review of all the major systems with an indication of their fields of greatest usefulness and with comments on both their desirable and undesirable features.

*A Dial Switching System for Toll Calls.*<sup>3</sup> HOWARD L. HOSFORD. At Philadelphia, on the night of August 21st and the early morning hours of August 22, 1943, the cutover of the new #4 System was no mere episode; it was one of the milestones of telephone history. Intertoll dialing in itself is not new but this joint project of the Bell Telephone Company of Pennsylvania and the Long Lines Department is especially significant as it has been designed so as to extend the field of toll dialing by the operators to include the largest cities and joins together various types of dialing equipment. In its scope this project includes many points in an area reaching from Richmond, Va. to New York City and from Harrisburg, Pa. to Atlantic City, N. J.

From a traffic standpoint the #4 toll switching system actually comprises

<sup>1</sup> *Jour. Applied Physics*, January 1944.

<sup>2</sup> *Jour. S. M. P. E.*, January 1944.

<sup>3</sup> *Bell Tel. Mag.*, Winter 1943-44.

three units, the switching equipment itself which is wholly mechanical, together with the so-called #4 and #5 switchboards. The #4 board is a cordless, key-typed call distributing board which is used in conjunction with the new switching system for such calls as must be given to an operator by offices not equipped for intertoll dialing. The operators at this board function as combined inward, through and tandem operators, thus eliminating the provision of separate units to provide these particular services. In brief, there is no basic difference between the essential operation of the #5 board and the conventional through board where delayed traffic is handled; however, operators handling calls at this board must make use of the new switching system to obtain both the calling and called offices by dialing.

Prior to the cutover the first trainees were given experience by handling some 300,000 test calls of every conceivable traffic characteristic. These were routed through the new system to break in the equipment and to shake down potential troubles. Two weeks prior to cutover a dress rehearsal was held, at which time about ten per cent of the circuits were put through their paces.

To provide information of value for future installations, arrangements were made for liberal provision of registers and meters to measure any and all phases of the various steps performed by the equipment. Some of these aids are not entirely new to telephone work but their application to toll, inward and through service is a departure.

The #4 System is running satisfactorily and both the equipment and the operators who use it deliver a high grade of service. Daily some 80,000 tandem, inward and through connections formerly handled by operators are routed through the equipment.

In connection with postwar planning, studies are now being made to determine future installations in order to take advantage of the possibilities of the new system. It is confidently expected that this will provide faster service on outward, inward and through calls and that transmission will be improved. These advantages should result in overall economies in outside plant and operating.

*Theoretical Limitation to Transconductance in Certain Types of Vacuum Tubes.*<sup>4</sup> J. R. PIERCE. The thermal-velocity distribution of thermionically emitted electrons limits the low-frequency transconductance which can be attained in tubes in whose operation space charge is not important. A relation is developed by means of which this dependence may be evaluated for tubes employing electric and magnetic control. This relation is applied to deflection tubes with electric and magnetic control and to stopping-

<sup>4</sup> *Proc. I. R. E.*, December 1943.

potential tubes. Magnetic control is shown to be inferior to electric control from the point of view of band-width and gain.

*Antenna Theory and Experiment.*<sup>5</sup> S. A. SCHELKUNOFF. This paper presents: (1) a comparison between several approximate theoretical formulas for the input impedance of cylindrical antennas in the light of available experimental evidence; and (2) a discussion of the local capacitance in the vicinity of the input terminals, mathematical difficulties created by its presence, and methods of overcoming these difficulties. No exact solution of the antenna problem is available at present and so far it is impossible to set definite limits for errors which may be involved in various approximations. For this reason in appraising these approximations one is forced to rely on one's judgment and on experimental evidence. It is hoped that this paper will aid in correlating theory and experiment to the advantage of both.

<sup>5</sup> *Jour. Applied Physics*, January 1944.

### Contributors to this Issue

H. J. MCSKIMIN, B.S. in Electrical Engineering, University of Illinois, 1937; M.S. in Physics, New York University, 1940. Bell Telephone Laboratories, 1937-. Engaged primarily in a study of electrical and electro-mechanical properties of piezoelectric crystals.

E. E. MOTT, Massachusetts Institute of Technology, B.S. 1927; M.S. 1928. General Electric Company, 1926-28. Bell Telephone Laboratories, 1928-. Mr. Mott has been engaged in telephone instruments research and development, particularly in connection with various types of telephone receivers and related devices. Since 1941 he has been engaged on war projects.

A. M. SKELLETT, A.B., 1924, M.S., 1927, Washington University; Ph.D., Princeton University, 1933; Instructor, 1927-28, Assistant Professor of Physics, 1928-29, University of Florida. Bell Telephone Laboratories 1929-. Dr. Skellett, formerly engaged in investigations pertaining to the transatlantic radio telephone, is concerned with applications of electronic and ionic phenomena.

R. A. SYKES, Massachusetts Institute of Technology, B.S. 1929; M.S. 1930. Columbia University, 1931-1933. Bell Telephone Laboratories, Research Department, 1930-. Mr. Sykes has been engaged in the applications of quartz crystals to broad-band carrier systems as filter and oscillator elements. Other work has included the application of coaxial lines as elements of filter networks and more recently the design and development of quartz crystals for radio frequency oscillators.